



Ana Cristina Dias da Mata

Licenciada em Ciências da Engenharia Química e Bioquímica

**The agroindustrial residue valorisation with
high pressure CO₂ within biorefinery
concept**

Dissertação para obtenção do Grau de Mestre em
Engenharia Química e Bioquímica

Orientador: Rafal Bogel-Lukasik

Presidente: Doutora Ana Aguiar Ricardo
Arguente: Doutora Susana Filipe Barreiros
Vogal: Doutor Rafal Bogel-Lukasik



FACULDADE DE
CIÊNCIAS E TECNOLOGIA
UNIVERSIDADE NOVA DE LISBOA

Março 2014

Ana Cristina Dias da Mata

Licenciada em Ciências da Engenharia Química e Bioquímica

**The agroindustrial residue valorisation with
high pressure CO₂ within biorefinery
concept**

Dissertação para obtenção do Grau de Mestre em
Engenharia Química e Bioquímica

Orientador: Rafal Bogel-Lukasik

Presidente: Doutora Ana Aguiar Ricardo
Arguente: Doutora Susana Filipe Barreiros
Vogal: Doutor Rafal Bogel-Lukasik



FACULDADE DE
CIÊNCIAS E TECNOLOGIA
UNIVERSIDADE NOVA DE LISBOA

Março 2014

“Copyright” Ana Cristina Dias da Mata, FCT/UNL e UNL

A Faculdade de Ciências e Tecnologia e a Universidade Nova de Lisboa têm o direito, perpétuo e sem limites geográficos, de arquivar e publicar esta dissertação através de exemplares impressos reproduzidos em papel ou de forma digital, ou por qualquer outro meio conhecido ou que venha a ser inventado, e de a divulgar através de repositórios científicos e de admitir a sua cópia e distribuição com objectivos educacionais ou de investigação, não comerciais, desde que seja dado crédito ao autor e editor.

Agradecimentos

Em primeiro lugar gostaria de agradecer ao Doutor Rafal Lukasik que se disponibilizou para me orientar durante a tese de mestrado. Pelas oportunidades proporcionadas ao longo deste período a nível profissional, pelos conhecimentos transmitidos, colaboração, paciência e disponibilidade para ajudar.

À Rita Morais pelo constante acompanhamento e ensinamentos durante esta fase. Pela ajuda que me deu sempre que precisei, pelo incentivo e positivismo sempre presentes.

Agradeço a todas as pessoas da Unidade de Bioenergia pela forma como fui recebida, e em especial à Sofia, Rita, André e Rute pela boa disposição, companheirismo, preocupação e pela disponibilidade para ajudar.

Um agradecimento muito especial ao Héber pelo carinho, amizade, confiança e incondicional apoio que sempre demonstrou.

Quero agradecer também à Sara, Margarida, Catarina, Liliana e Tiago pela amizade, apoio e bons momentos partilhados ao longo destes anos de faculdade.

Não podia deixar de agradecer à minha família, principalmente aos meus pais, irmão e avós, que me acompanharam durante este período. Agradeço-vos pela ajuda, paciência e incentivo.

Abstract

Wheat straw is an agricultural residue with low commercial value and is the second most abundant raw material in the world.

With the aim of its valorisation within a biorefinery concept, the effect of high pressure CO₂-H₂O approach on the xylo-oligosaccharides production and on the digestibility of cellulose was studied. The parameters studied in the high-pressure CO₂-H₂O reactions were temperature (35, 130, 215 and 225°C), pressure of CO₂ (0, 15, 30, 45 and 54 bar), biomass loading (150 g of H₂O·15 g dry wheat straw⁻¹ and 100 g of H₂O·10 g dry wheat straw⁻¹) and time of reaction (0, 30, 60, 90 and 180 min).

It was found that *in situ* formed carbonic acid enhanced hydrolysis of major hemicellulose compound - xylan to xylo-oligosaccharides since an increase of 45% of xylo-oligosaccharides yield was observed when comparing autohydrolysis with CO₂-H₂O approach. The physical and chemical effect of CO₂ presence also enhances the enzymatic digestibility of cellulose. It was obtained an 82% glucan to glucose yield with 54 bar of CO₂ that corresponds to a 26% improvement when comparing it with the autohydrolysis processed straw. FT-IR analysis was employed to study the compositional changes regarding cellulose crystallinity and the SEM measurements allowed the analysis of the effect of high-pressure CO₂-H₂O on morphology of the solid residue.

Keywords: CO₂, high pressure, xylo-oligosaccharides, enzymatic hydrolysis, glucose, wheat straw

Resumo

A palha de trigo é um resíduo agrícola de baixo valor comercial sendo a segunda matéria-prima mais abundante a nível mundial.

Com o objectivo da valorização da palha de trigo, integrada no conceito de biorefinaria, foi estudado o efeito do sistema $\text{CO}_2\text{-H}_2\text{O}$ a altas pressões como pré-tratamento na produção de xilo-oligossacáridos e na digestibilidade enzimática da celulose. Os vários parâmetros estudados foram a temperatura (35, 130, 215 e 225°C), pressão (0, 15, 30, 45 e 54 bar), quantidade de água e biomassa adicionada ao reator (100 g de água·10 g de palha de trigo⁻¹ e 150 g de água·15 g de palha de trigo⁻¹) e o tempo de reacção (0, 30, 60, 90 e 180 minutos).

Verificou-se que o ácido carbónico formado em solução melhorou a hidrólise do xilano, contido na hemicelulose, a xilo-oligossacáridos pois foi observado um aumento de 45% do rendimento em xilo-oligossacáridos quando comparando a autohidrólise ao pré-tratamento com $\text{CO}_2\text{-H}_2\text{O}$. O efeito químico e físico da presença do CO_2 também mostrou melhorar a digestibilidade enzimática da celulose. Foi obtido um rendimento de conversão de glucano a glucose de 82% com 54 bar de CO_2 , o que corresponde a uma melhoria de 26% quando comparando à palha processada por autohidrólise.

A análise por FT-IR foi empregue para estudar as alterações composicionais relacionadas com a cristalinidade da celulose e as medições por SEM permitiram a análise do efeito do pré-tratamento na morfologia do resíduo sólido.

Palavras-chave: CO_2 , alta pressão, xilo-oligossacáridos, hidrólise enzimática, glucose, palha de trigo.

List of Publications

The results presented in this thesis were submitted for publication in the following work: Integrated conversion of agroindustrial residue with high pressure CO₂ within biorefinery concept, Green Chemistry, 2014 and presented during the oral presentation at the Meeting of the COST Action EUBiS TD1203 Food Waste Valorisation for Sustainable Chemicals, Materials and Fuels (EUBiS) held in Toulouse, France (2014).

List of Contents

AGRADECIMENTOS	III
ABSTRACT	V
RESUMO	VII
LIST OF PUBLICATIONS	IX
LIST OF FIGURES	XIII
LIST OF TABLES	XV
NOMENCLATURE	XVII
1. INTRODUCTION	1
1.1. GREEN CHEMISTRY	1
1.2. LIGNOCELLULOSE BIOMASS	2
1.3. BIOMASS PRE-TREATMENTS	6
1.3.1. <i>Pre-treatment products</i>	8
1.4. HIGH DENSITY FLUIDS	9
1.5. ENZYMATIC HYDROLYSIS	11
2. OBJECTIVES	13
3. MATERIALS AND METHODS	15
3.1. MATERIALS	15
3.2. HIGH PRESSURE CO ₂ -H ₂ O PRE-TREATMENT OF WHEAT STRAW	15
3.3. CHEMICAL ANALYSES	17
3.3.1. <i>Solids moisture determination</i>	17
3.3.2. <i>Liquors dry weight determination</i>	17
3.3.3. <i>Characterisation of the feedstock material composition</i>	17
3.3.4. <i>Characterisation of the processed solids</i>	18
3.3.5. <i>Liquor and post-hydrolysate characterisation</i>	18
3.4. GAS PHASE	18
3.5. FT-IR MEASUREMENT OF CELLULOSE CRYSTALLINITY	18
3.6. SEM ANALYSIS	19
3.7. ENZYMATIC HYDROLYSIS	19
3.7.1. <i>Characterisation of the samples composition</i>	20
3.8. QUANTIFICATION OF TOTAL PHENOLICS	20
4. RESULTS AND DISCUSSION	21
4.1. CHEMICAL COMPOSITION OF WHEAT STRAW	21

4.2.	HIGH-PRESSURE CO ₂ -H ₂ O	21
4.2.1.	<i>Effect of reaction severity on pre-hydrolysate composition</i>	21
4.2.2.	<i>Hydrolysate pH</i>	27
4.2.3.	<i>Effect of reaction severity on gas phase composition</i>	28
4.2.4.	<i>Effect of severity on solid phase composition</i>	29
4.2.5.	<i>Characterisation of cellulose crystallinity of pre-treated solids</i>	30
4.2.6.	<i>Effect of high-pressure CO₂-H₂O on morphology of wheat straw</i>	32
4.2.6.1.	Scanning Electron Microscopy	32
4.3.	ENZYMATIC HYDROLYSIS OF PRE-TREATED SOLIDS	34
4.3.1.	<i>Effect of CO₂ pressure</i>	34
4.3.2.	<i>Effect of temperature</i>	36
4.3.3.	<i>Effect of reaction time</i>	38
4.3.4.	<i>Effect of CO₂/dry biomass ratio</i>	39
4.4.	PROCESS OVERVIEW.....	40
5.	CONCLUSIONS AND OUTLOOK	43
5.1.	PERSPECTIVES	44
6.	REFERENCES	45
7.	APPENDIX	53
	ANNEX A – DETERMINATION OF THE PARTIAL PRESSURE OF CO ₂	53
	ANNEX B – DATA FOR THE DETERMINATION OF CO ₂ DENSITY	54
	ANNEX C – DETERMINATION OF FEEDSTOCK AND SOLID RESIDUES	54
	ANNEX D – DETERMINATION OF PERCENT DIGESTIBILITY OF CELLULOSE	55
	ANNEX E – PHENOLICS CONCENTRATION DETERMINATION	56

List of Figures

Figure 1.1 – Wheat straw biorefinery concept. Adapted from ⁹	2
Figure 1.2 – Spatial arrangement of cellulose hemicellulose and lignin in the cell walls of lignocellulosic biomass. ¹³	3
Figure 1.3 – (A) Hydrophilic and hydrophobic sites of cellulose. (B) Schematic drawing of the intrasheet hydrogen-bonding network in cellulose. ²¹	4
Figure 1.4 – Hexoses and pentoses typically found in hemicellulose. ¹³	5
Figure 1.5 – The three lignin monolignols. ¹³	5
Figure 1.6 – Effect of pre-treatment in the structure of lignocellulosic biomass. Adapted from ¹⁷	6
Figure 1.7 – Degradation products of cellulose, hemicellulose and lignin. ⁴²	9
Figure 1.8 – CO ₂ pressure-temperature phase diagram. ⁴⁹	9
Figure 1.9 – Cellulose depolymerization by cellulases. ⁵⁷	12
Figure 3.1 – Scheme of the high pressure CO ₂ -H ₂ O pre-treatment apparatus.....	16
Figure 4.1 – Content in furfural (g·L ⁻¹) of the recovered gas phase as a function of number of moles of CO ₂ . 150/15 and 100/10 represent the ratio between mass of water and mass of biomass.	28
Figure 4.2 – Composition of the solids and solid yield obtained after high-pressure CO ₂ -H ₂ O	30
Figure 4.3 – The FT-IR spectra of untreated (black line), autohydrolysis (red line) and CO ₂ processed wheat straw (green line) showing the regions for LOI determination.	31
Figure 4.4 – SEM images of untreated wheat straw (A,B), autohydrolysis (C,D) and treated at 225°C with 45 bar of CO ₂ (E,F).....	33
Figure 4.5 – Effect of CO ₂ pressure of high-pressure CO ₂ -H ₂ O on enzymatic hydrolysis yield	34
Figure 4.6 – The schematic representation of both physical and chemical effect of high pressure processes of wheat straw valorisation.....	36
Figure 4.7 – Effect of temperature of high-pressure CO ₂ -H ₂ O on enzymatic hydrolysis.	37
Figure 4.8 – Effect of CO ₂ /biomass mass ratio on glucose yield.	39
Figure 4.9 – The mass balance of integrated polysaccharide conversion.	40
Figure 4.10 – Mass balance of xylan and glucan within the overall process for the autohydrolysis pre-treatment.....	40
Figure 7.1 – Values for Henry's constant.	53

List of Tables

Table 1.1 – Typical chemical composition of various lignocellulosic materials. ¹⁶	3
Table 1.2 – Range of thermophysical properties of gases, supercritical fluids and liquids. ⁴⁹	10
Table 1.3 – Critical parameters of several fluids ⁴⁹	10
Table 4.1 – Macromolecular composition of wheat straw (% of dry weight)	21
Table 4.2 – Composition of liquors ($\text{g}\cdot\text{L}^{-1}$) of each product present in the liquors ($\text{g}\cdot 100\text{ g}^{-1}$ of the initial amount present in the feedstock) obtained after high-pressure $\text{CO}_2\text{-H}_2\text{O}$ of wheat straw at 130°C	25
Table 4.3 – Composition of liquors ($\text{g}\cdot\text{L}^{-1}$) of each product present in the liquors ($\text{g}\cdot 100\text{ g}^{-1}$ of the initial amount present in the feedstock) obtained after high-pressure $\text{CO}_2\text{-H}_2\text{O}$ of wheat straw at 215°C and 225°C	26
Table 4.4 – The LOI index for untreated, autohydrolysis and CO_2 -treated wheat straw.....	31
Table 7.1 – Data for determination of density of CO_2 using the PR-EOS equation, as well as the number of moles of CO_2	54

Nomenclature

A	Absorbance
AcOS	Acetyl groups bounded to oligosaccharides
AFEX	Ammonia fiber explosion
Arn	Arabinan
Ara	Arabinose
CP	Critical point
CS_{pCO_2}	Combined Severity factor
DP	Degree of polymerization
FT-IR	Fourier Transform Infrared Spectroscopy
FPU	Filter paper units
F	Correction factor
GlcOS	GlucO-oligosaccharides
Gn	Glucan
Glc	Glucose
GAc	Acetyl groups
HPLC	High Pressure Liquid Chromatography
HMF	5-Hydroxymethylfurfural
kg	Kilogram
keV	Electronvolt
K	Kelvin
k_H	Henry's constant
R_0	Severity factor
L	Liter
LK	Klason Lignin
LOI	Lateral Order Index
m	Meter
MPa	Mega Pascal

M	Molar
min	Minute
MΩ	Megaohm
NREL	National Renewable Energy Laboratory
n	moles
N	Normality (concentration)
OS	Oligosaccharides
pNPGU	p-nitrophenyl-β-D-galactopyranoside units
p _{CO₂}	pressure of carbon dioxide
p _{CO₂initial}	initial pressure of CO ₂ in the beginning of reaction
p _{CO₂final}	final pressure of CO ₂ in the reaction
p	Pressure
p _c	Critical pressure
PR-EOS	Peng-Robinson equation of state
AIR	Acid insoluble residue weight
rpm	Rotations per minute
R	Gas constant
SY	Solid Yield
scCO ₂	Supercritical carbon dioxide
SCF	Supercritical fluids
SEM	Scanning Electron Microscopy
t	Time
T	Temperature
T _c	Critical temperature
T ₀	Initial temperature
TP	Triple point
UV/Vis	Ultraviolet/visível
v	Volume
w	Weight
w _{sol}	Solution weight

XOS	Xylo-oligosaccharides
x	mole fraction
Xn	Xylan
Xyl	Xylose
€	Euro
∅	Diameter
ρ	Density
ω	Acentric factor

1. Introduction

1.1. Green Chemistry

Green chemistry is a recent field of chemistry with the purpose of introducing clean processes in chemical manufacturing industries. It is defined as the “design of chemical products and processes to reduce or eliminate the use and generation of hazardous substances”.¹ Green chemistry is governed by 12 principles established by Anastas and Warner²: (a) prevention, (b) atom economy, (c) less hazardous chemical syntheses, (d) design for safer chemicals, (e) safer solvents and auxiliaries, (f) design for energy efficiency, (g) use of renewable feedstocks, (h) reduction of derivatives, (i) catalysis, (j) design for degradation, (k) real-time analysis for pollution prevention and (l) inherently safer chemistry for accident prevention. The mentioned principles are guidelines for the development of alternative processes which should be applied to whole lifecycle of a product.¹ An ideal process should use non-polluting feedstocks, generate no secondary products and require no solvents for the chemical conversion, or to isolate and purify the product.³ The main objective of green chemistry is to achieve sustainable development, in other words, it aims to fulfill the needs of the present society without compromising the ability of the future generations to meet their own needs.⁴

Today's economy and lifestyle are strongly dependent on fossil fuels.⁵ However their intense use, non-renewable nature and limited reservoir will inevitably lead to its depletion, thus searching for another resources is urgent.⁶ Besides oil feedstock availability, there is also the environmental aspect which is likewise a driver into shifting resources' feedstocks to more sustainable alternatives.^{4,5}

Biomass is the only viable alternative to fossil fuels since, in addition to them, is the only rich source of carbon with a lifespan measured in years, that is much shorter than that for fossil fuels (hundreds of millions of years).^{4,5} The use of biomass fits in the ambit of a biorefinery. A biorefinery is a concept analogous to a petroleum refinery.⁷ It is a facility that uses biomass as input with the objective of converting it into materials, value-added products, fuels and energy, through the combination of diverse technologies.⁸ However, the use of a sustainable feedstock, such as biomass, is not sufficient to ensure a sustainable future, and that is why integration of green chemistry with biorefineries is required.⁴ The application of green technologies to the transformation of low value and widely available biomass feedstocks allows the development of sustainable chemicals and materials.⁵

Unlike oil, biomass has diverse composition depending on species, climacteric conditions and many others variables. Therefore, for an economic and technological feasibility, a biorefinery must be able to process different feedstocks with different composition.⁴ Thus an integrated production of value-added products, materials and energy (biofuels) may provide economic, energetic and social feasibility to the biorefinery.⁸

Figure 1.1 provides an example of an agricultural by-product (wheat straw) that can be the basis of a biorefinery since it's possible to obtain a variety of value-added biochemical, materials and also biofuels from it.⁹

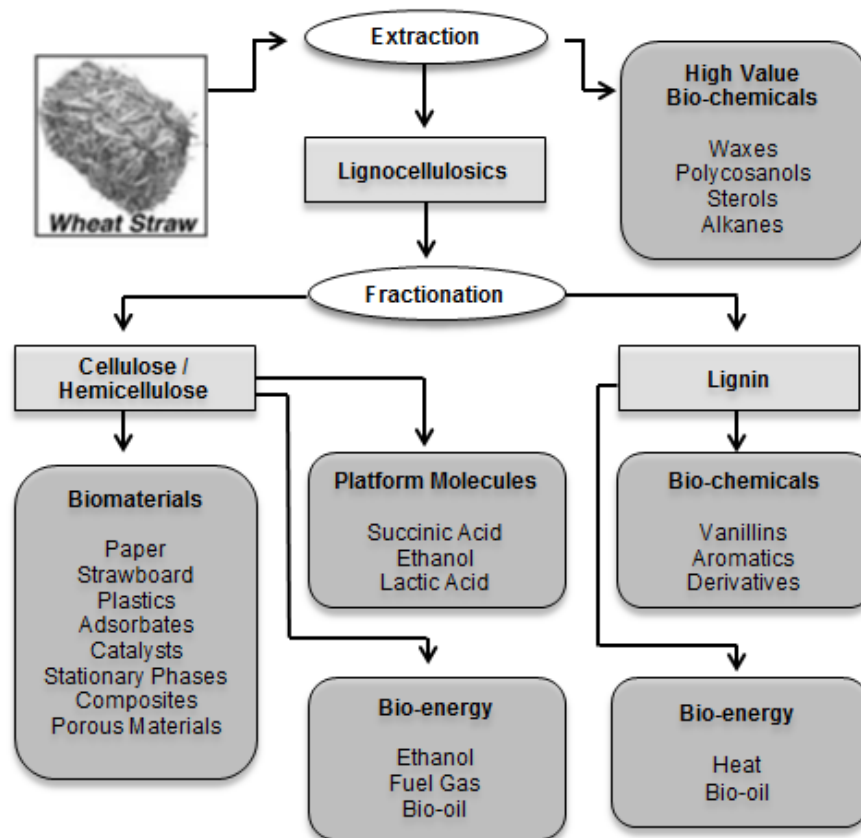


Figure 1.1 – Wheat straw biorefinery concept. Adapted from⁹

The biorefinery concept can be accomplished through two main platforms, thermochemical and biochemical. The biochemical platform consists in variety of processes such as extraction, separation and biological conversion of biomass into biofuels, biomaterials and biochemicals. The thermochemical platform produces syngas or bio-oil through thermal treatment processes, that after can be converted into energy, fuels, materials and chemicals.^{8,10}

1.2. Lignocellulose Biomass

Lignocellulose is a renewable organic material, whose wastes are produced in large amounts in different areas including forestry (treetops, branches), agriculture (straw, stover) and food (peanut shells, rice husks) industrie.¹¹ Chemical composition of lignocellulosic feedstock is often a barrier limiting the complete valorisation of biomass.¹² Lignocellulosic materials are majority composed by two polymeric carbohydrates, (cellulose and hemicellulose) and lignin, an aromatic polymer (Figure 1.2).¹³ The mutual interactions create an intricate and recalcitrant to deconstruction structure.^{14,15} Additionally, the lignocellulosic feedstock contains pectins, inorganic compounds, proteins and extractives, such as waxes and lipids in lesser amounts.¹³

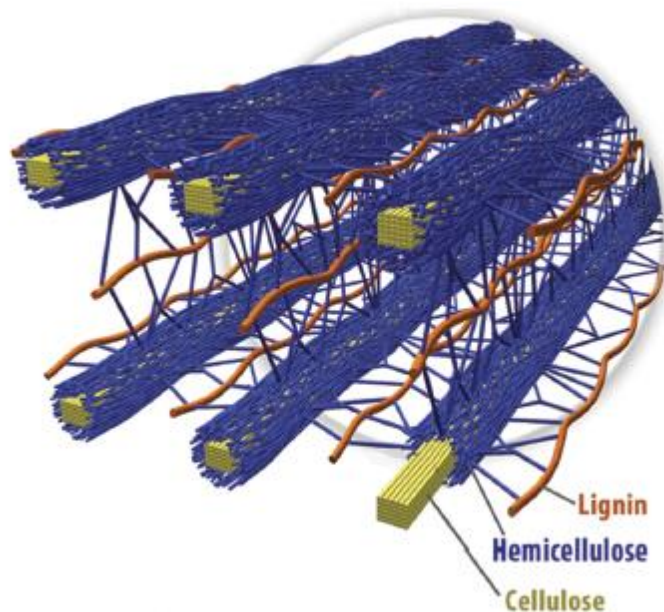


Figure 1.2 – Spatial arrangement of cellulose hemicellulose and lignin in the cell walls of lignocellulosic biomass.¹³

As it was aforementioned the chemical composition of biomass depends on many variables and examples are given in Table 1.1.¹⁶

Table 1.1 – Typical chemical composition of various lignocellulosic materials.¹⁶

Raw material	Lignin (%)	Cellulose (%)	Hemicellulose (%)
Hardwoods	18 - 25	45 - 55	24 - 40
Softwoods	25 - 35	45 - 50	25 - 35
Grasses	10 - 30	25 - 40	25 - 50

Cellulose, the main component of lignocellulosic biomass, is a homopolymer consisting of D-glucose units linked together by β -(1,4)-glycosidic bonds which results in a linear glycan chain.^{17,18} The basic repeating unit is cellobiose which is a disaccharide of D-glucopyranose.¹⁹ Cellulose chains have a degree of polymerisation with a range of 500 to 25000.¹⁶ The hydrogen bonds present in the cellulose structure allow the formation of microfibrils that consists of cellulose chains packaged together, with amorphous and crystalline regions.²⁰

As presented in Figure 1.3, the hydroxyl groups in cellulose structure are in equatorial positions that help to create hydrogen bonds between molecules that are in the same crystal layer, thus giving to the side chains of cellulose an hydrophilic nature. However, the same does not occur for upper and bottom layers, in which hydrogen atoms are in axial positions preventing the formation of these bonds,

thus giving to these regions a hydrophobic nature. These hydrophobic spots must contribute to the insolubility of cellulose under normal conditions.¹⁹

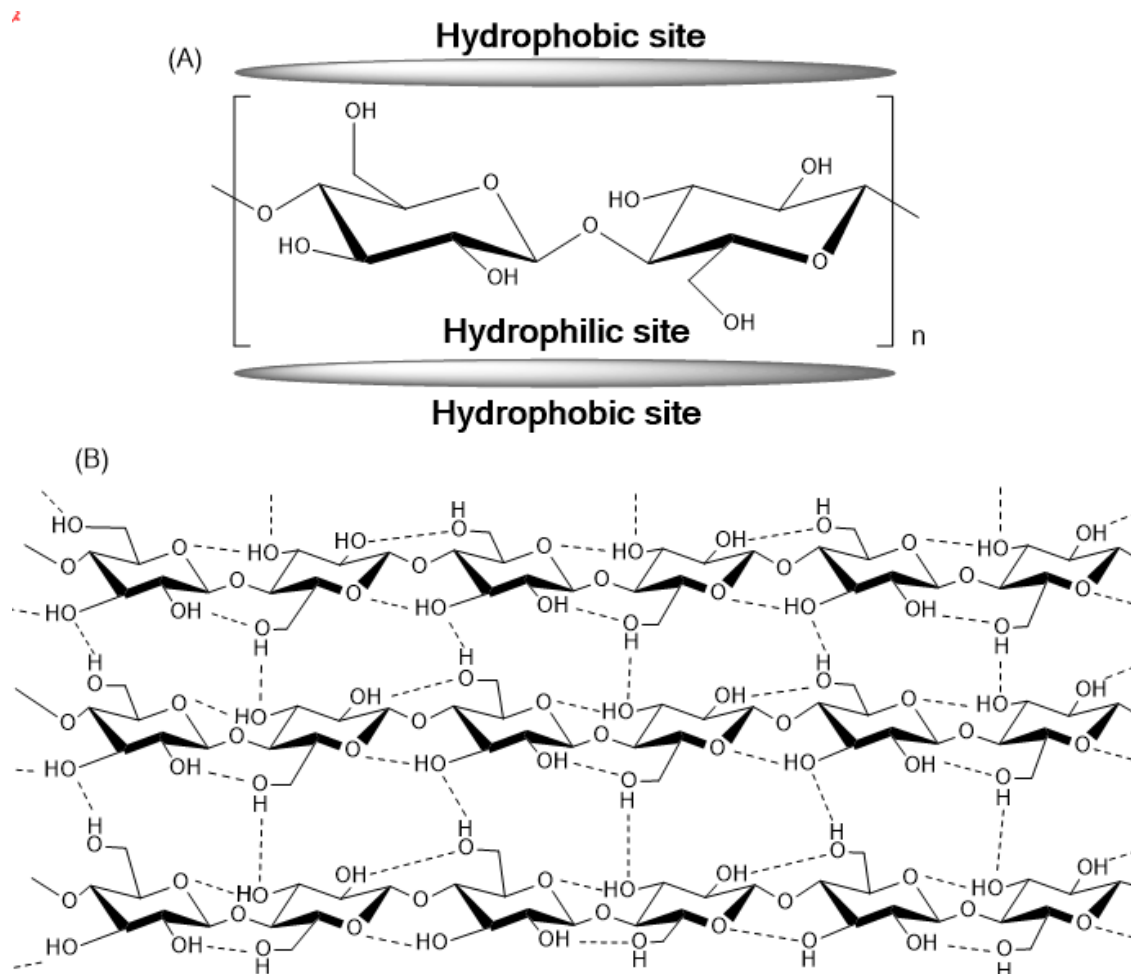


Figure 1.3 – (A) Hydrophilic and hydrophobic sites of cellulose. (B) Schematic drawing of the intrasheet hydrogen-bonding network in cellulose.²¹

Hemicelluloses are a heterogeneous class of polymers that contains pentoses (xylose and arabinose), hexoses (glucose, galactose and mannose), as can be seen in Figure 1.4., and also branched groups such as acetyl and methyl groups and cinnamic, glucuronic and galacturonic acids.¹³ These polymers are classified accordingly to the main sugar residue present in the backbone, which include for example, mannans, glucans and xylans, the last two being the most prevalent.¹⁹ The fact that they present a low degree of polymerization (100-200)¹³ and a branched structure provides them an amorphous nature and therefore, are generally much easily hydrolysed in comparison with cellulose.^{13,22}

The degree of substitution and the kind of substituents' groups vary with plant species. For example in hardwoods, xylan is highly acetylated and branched with small amounts of uronic acid, while in softwoods, it is partially acetylated and branched with arabinose and uronic acid.¹⁷ Hemicelluloses are non-covalently bounded to cellulose fibrils¹³ and their side groups have a great importance in their binding to lignin.¹⁹ Lignin helps maintaining these three polymers cohesive.¹³

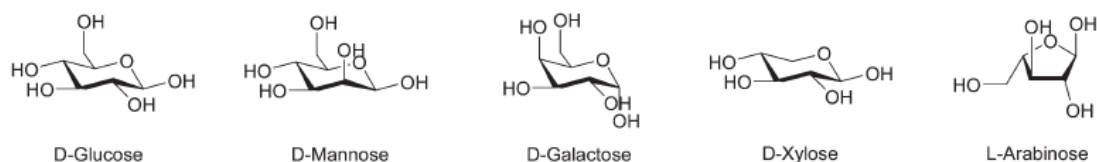


Figure 1.4 – Hexoses and pentoses typically found in hemicellulose.¹³

Lignin is an aromatic, heterogeneous polymer, biosynthesised from three phenylpropanoids precursors: coniferyl, sinapyl and p-coumaryl alcohols which when integrated in lignin polymer are called guaiacyl, syringyl and p-hydroxyphenyl respectively, (Figure 1.5) according to their aromatic ring. The composition of lignin varies between hardwoods, softwoods and grasses, which has great effect on biomass deconstruction.¹³

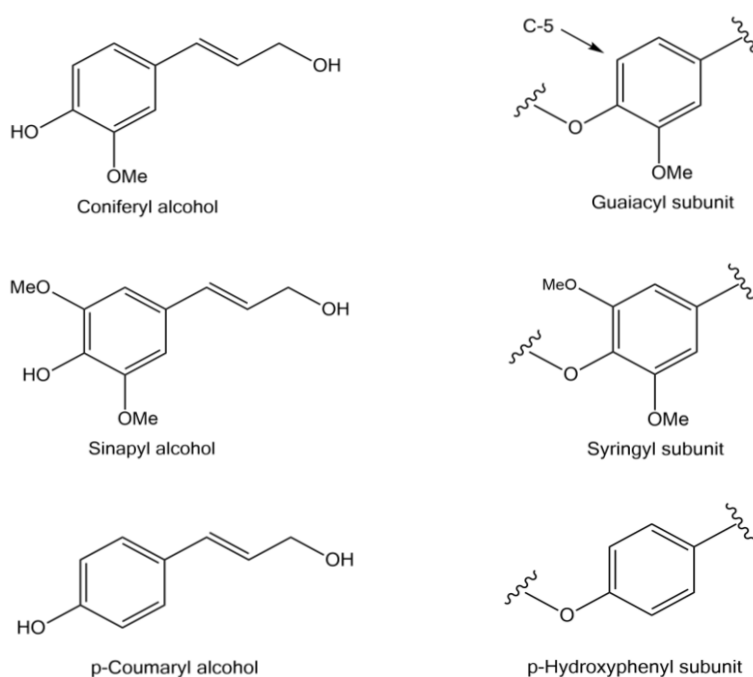


Figure 1.5 – The three lignin monolignols.¹³

Wheat straw is an agricultural residue with low commercial value and it consists in the leftover canes after the wheat grains are harvested.²³ It is the most abundant raw material in Europe and the second most abundant in the world, with an annual production of 534.23 million tons in 2011.²⁴ Nowadays, 21% of world's food depends on wheat and with growth of population it's expected that wheat production increases, thus giving wheat straw great potential as feedstock for various end-uses.²⁵ Its applications include also a fermentation industry (biofuel and hydrolytic enzymes production), pulp and paper industry, bioremediation (as a substrate for sorption of heavy metals), soil fertility and organic content, medicinal value (prevents tooth disorders), among others.^{26,27}

1.3. Biomass pre-treatments

A variety of factors in the lignocellulosic structure of biomass influences the capacity of their conversion into valuable products.¹² Crystallinity of cellulose, degree of polymerization, moisture content, available surface area or lignin content are some of factors constituting a barrier for the conversion of these materials.^{28,29} To overcome these problems, it is necessary to introduce an intermediate step, named pre-treatment, with the focus on altering or removing structural and compositional impediments for hydrolysis.^{12,28} A schematic representation of the pre-treatment effect on the lignocellulosic structure is shown in Figure 1.6.

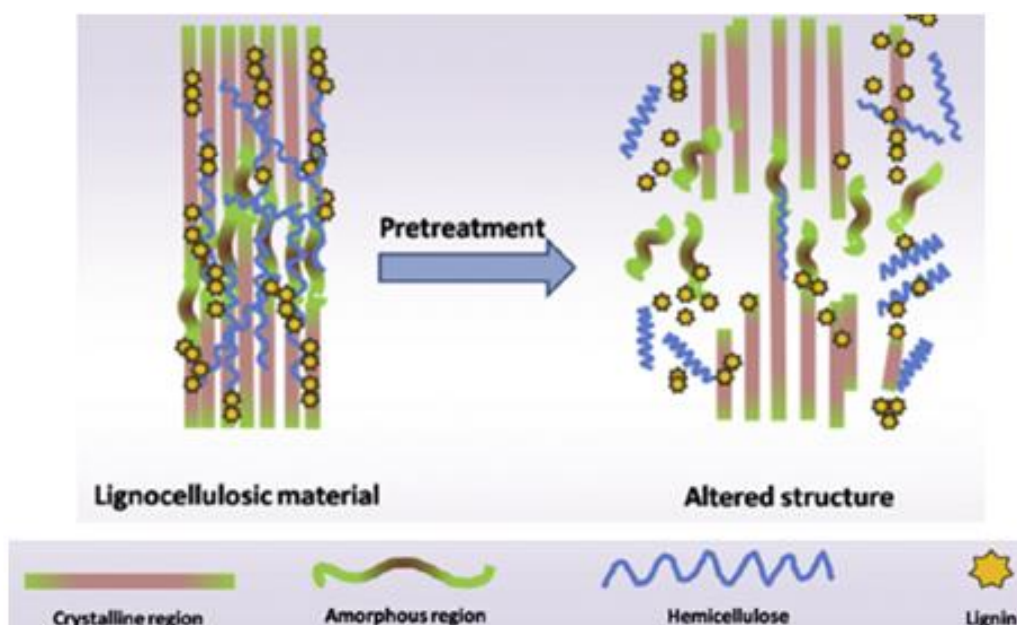


Figure 1.6 – Effect of pre-treatment in the structure of lignocellulosic biomass. Adapted from ¹⁷

The desired pre-treatment process should (i) produce highly digestible solids, enhancing sugar yields during enzyme hydrolysis, (ii) avoid degradation of sugars, (iii) minimise the formation of inhibitors for subsequent fermentation steps, (iv) be cost effective by operating in reactors of moderate size and (v) minimise heat and power requirements.^{17,30}

Pre-treatment methods can be divided in physical, chemical, physico-chemical and biological techniques.^{18,28} Physical pre-treatments refer to the size reduction of biomass particles leading to the increase of surface area. Moreover, it guides to a decrease of degree of polymerisation and sometimes to the decrystallisation of the lignocellulosic structure.¹⁸ Mechanical comminution (chipping, milling and grinding), and microwave treatment are examples of these kind of pre-treatments.^{18,28,31}

Biological or microbial pre-treatment uses microorganisms to convert biomass into more accessible compounds for hydrolysis.¹⁸ Diluted or concentrated acid, alkali, organosolv, oxidative and ionic liquids are some of the methods recognised as chemical pre-treatments.³¹ This class of pre-treatments involves the addition of chemicals whose choice depends on pre-treatment objectives. An acid catalysed process, usually H_2SO_4 , has generally two different approaches based on the concentration

of the acid present.¹⁴ The concentrated-acid processes operate at low temperatures with acid concentrations of 72% H₂SO₄ whilst dilute-acid processes use high temperatures, concentrations in the range 0.5-1.5% and requires a two-step hydrolysis.¹⁴ In an alkaline hydrolysis it is believed that a saponification reaction occurs, which leads to the cleavage of the intermolecular ester bonds crosslinking xylan, hemicellulose and other components.^{29,32} Sodium hydroxide and lime are bases that showed to be effective to disrupt the lignin structure.³³ In organosolv method an organic solvent mixture with inorganic acid catalysts (H₂SO₄, HCl) is used to break the internal lignin and hemicellulose bonds. Methanol, ethanol, acetone and ethylene are some of the organic solvents employed in this technique.^{12,31}

Ionic liquids are a class of solvents used in pre-treatments relatively recently.^{33,34} These green solvents are composed of ions with countless combinations of cations and anions, allowing them to be adapted to increase their power of dissolution of carbohydrates.³⁵

Within the physico-chemical class of pre-treatments, the processes that uses both physical and chemical effects in order to break the structure of the lignocellulosic material are included.³⁰ In an explosion pre-treatment a gaseous substance (steam, CO₂) is introduced in the system and high pressures and temperatures (160 to 260°C) are applied for a determined period of time (seconds to minutes), after which an explosive release of the pressure occurs.³⁶ The rupture of the linked acetyl groups with hemicelluloses generates acetic acid and the acidic nature of water at high temperatures,¹⁸ promotes hydrolysis of hemicelluloses and breaks down the glycosidic bonds between hemicellulose and cellulose. This process represents the chemical technique whilst the physical one comes from the rapid decompression of the system where expansion causes the vaporisation of saturated fluid within the fibrils, breaking down the molecular linkages.³⁰ In ammonia fiber explosion (AFEX) the material is subjected to liquid ammonia-water mixtures under high pressures and moderate temperatures (90 to 100°C) prior to rapid depressurisation.^{37,36,38} Liquid hot water, also known as autohydrolysis or subcritical pre-treatment, uses high temperatures and pressures to keep water in the liquid state to dissolve hemicellulose leaving cellulose more accessible.^{29,36,38} Autohydrolysis pre-treatment consists in reactions between the hydronium ions generated from water and acetic acid groups released from hemicelluloses and the glycosidic bonds of lignocellulose.^{36,38,39} The conversion of polysaccharides into oligomers and, at less extent, into monomers is the result of these reactions.³⁹ The nature of autohydrolysis provides lower by-products generation and minor problems related to equipment corrosion.⁴⁰

Supercritical carbon dioxide as a pre-treatment has been increasingly studied due to the properties of fluid acquired when critical pressure and temperature are attained. The simultaneous liquid-like solubilities and gas-like diffusivities gives the ability to penetrate into the crystalline structure of lignocelluloses.³⁰ When combined with water, CO₂ acts as a catalyst due to the formation of carbonic acid, which promotes the biomass hydrolysis and also has a swelling effect on biomass.^{18,30,41} Furthermore, the employment of CO₂ usually allows to reduce the temperature of the process leading to minor degradation of monomers increasing the yield of the reaction.¹⁴ Additional benefit is the fact that CO₂ can be easily removed from the system by depressurisation leaving no waste products due to

almost complete immiscibility in water at atmospheric conditions.^{18,41} It is important to note that in CO₂ explosion biomass is subjected to explosive decompression while in water-CO₂ pre-treatment a slow depressurisation occurs.

1.3.1. Pre-treatment products

Several compounds can result from the hydrolysis of hemicellulose such as pentose and hexose sugars (either in oligomer or monomer form), aliphatic acids (acetic, formic and levulinic) and furan aldehydes (5-hydroxymethylfurfural and furfural). Lignin and cellulose mostly remain as a solid residue, although minor part of it is degraded to phenolics and other aromatic compounds and gluco-oligosaccharides (GlcOS) respectively.⁴²

Xylo-oligosaccharides (XOS) are sugar oligomers produced during the hydrolysis of xylan, the major component of plant hemicelluloses.⁴³ They are formed by xylose units with a varying structure depending on degree of polymerization, monomeric units and types of linkages. The number of xylose residues forming the structure can vary from 2 to 10, and they are linked through β -(1-4)-linkages. In addition to xylan, side groups such as α -D-glucopyranosyl, uronic acid, acetyl groups or arabinofuranosyl residues may be present, providing XOS diverse biological properties. At industrial scale, XOS are produced from xylan-rich lignocellulosic materials (straw, bagasse, corn cobs) and enzymatic and chemical methods or a combination of both of them.⁴⁴ Oligosaccharides have been a subject of special interest due to their prebiotic properties. They present physiological importance such as, reducing cholesterol level, maintaining the gastrointestinal health, improving the biological availability of calcium, among others.⁴³ XOS applications includes food (antiobesity diets), pharmaceutical (prevention and treatment of gastrointestinal infections), feed (for domestical animals) or agricultural (Growth stimulator and accelerator) fields.⁴⁵ In addition they also have important physico-chemical properties which include stability over a wide range of pH and temperatures, sweetener, retain the moisture of food and control the microbial activity as well.^{46,47} XOS have an estimated market price of 16€/kg which makes them potential value-added products from agricultural waste.⁴⁶

The acetic, formic and levulinic acids are present in the lignocellulose hydrolysates. Acetic acid is formed by hydrolysis of acetyl groups of hemicellulose. Formic acid is the degradation product of furfural while levulinic acid is a degradation product of both furfural and 5-hydroxymethylfurfural (HMF). Furfural and HMF are furan aldehydes produced by the dehydration of pentose and hexose sugars, respectively, and lignin is the main source of phenolic compounds.⁴² Figure 1.7 presents a scheme with the main routes of formation of these products.

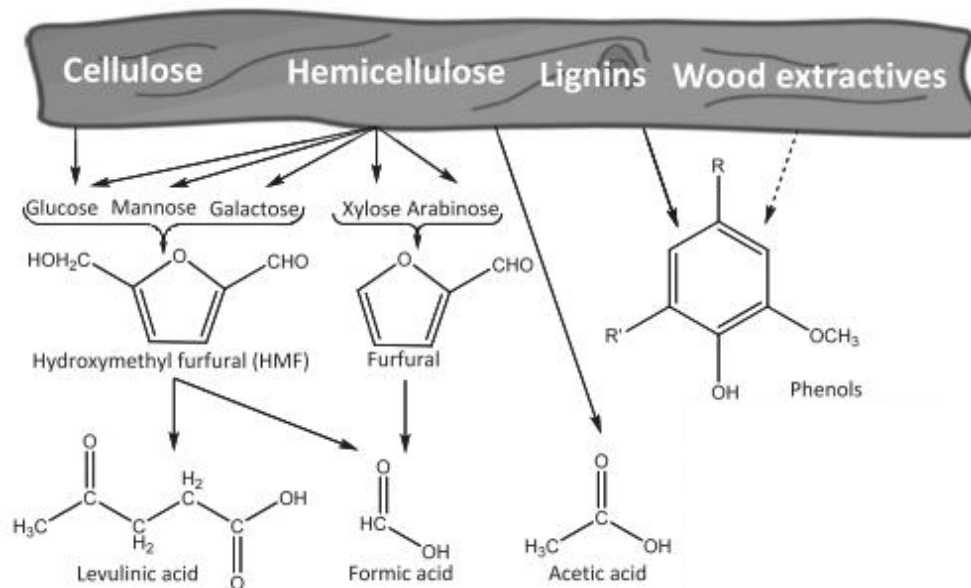


Figure 1.7 – Degradation products of cellulose, hemicellulose and lignin.⁴²

1.4. High density fluids

Supercritical fluids (SCF) are gases above their critical temperature and pressure.⁴⁸ Figure 1.8 presents a CO₂ pressure-temperature phase diagram, showing the critical point (CP) where the distinction between gas and liquid ceases.⁴⁹ Correspondent values of temperature and pressure are designated by critical pressure and critical temperature.⁴⁹

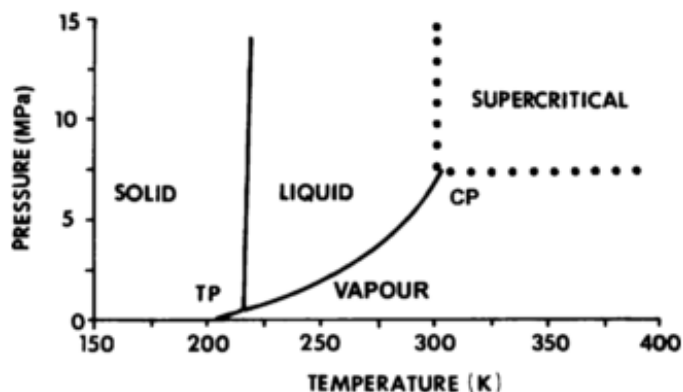


Figure 1.8 – CO₂ pressure-temperature phase diagram.⁴⁹

One of the main characteristics of supercritical fluids is that they possess simultaneously properties of liquids and gases, that is, they have gas-like mass transfer properties and liquid-like solvent power. Their high diffusivities make them easier to penetrate in solid materials and the fact that they present a very low superficial tension, allows them to infiltrate in low porosity materials. In addition to these characteristics they also exhibit low viscosity, which is favourable to their movement.⁴⁸

Typical density, viscosity and diffusion values of liquids, gases and supercritical fluids are listed in Table 1.2. As it can be seen, the transport properties such as viscosity and diffusion of a supercritical fluid are between those of liquids and gases. This indicates that these fluids are capable for a faster and deeper penetration into a solid matrix. Also, their intermediate densities points to a similar solvent power to those of liquids.^{48,49,50} Furthermore, their dissolution power is controllable through temperature and pressure variations close to the critical region.^{49,51}

Table 1.2 – Range of thermophysical properties of gases, supercritical fluids and liquids.⁴⁹

Fluid state	Density (g·L)	Diffusion coefficient (m²·s)	Viscosity (kg·m⁻¹·s⁻¹)
Gas	1 - 100	10 ⁻⁴ - 10 ⁻⁵	10 ⁻⁵ - 10 ⁻⁴
Supercritical fluid	250 - 800	10 ⁻⁷ - 10 ⁻⁸	10 ⁻⁴ - 10 ⁻³
Liquid	800 - 1200	10 ⁻⁸ - 10 ⁻⁹	10 ⁻³ - 10 ⁻²

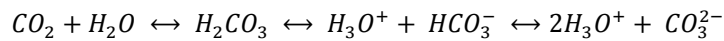
Carbon dioxide is probably the most commonly used SCF because it is a non-flammable, non-corrosive, cheap gas and can be obtained in large scale with diverse purity grade.^{48,50} Furthermore, among the various supercritical fluids listed in Table 1.3, carbon dioxide has the critical point easily achievable at the industrial conditions.

Table 1.3 – Critical parameters of several fluids⁴⁹

Fluid	T_c (°C)	P_c (bar)
Ethylene	9.25	50.4
Carbon dioxide	30.95	73.8
Ethane	32.25	48.8
Nitrous oxide	36.45	72.4
Propane	96.65	42.5
Ethanol	240.75	61.4
Benzene	288.95	48.9
Toluene	318.65	41.0
Water	401.15	221.2

Working with fluids in their supercritical region or closed to it provides advantages due to properties acquired in that circumstances. When joining CO₂ and water, interaction between them origins in the formation of carbonic acid according to equation 1.1.⁵²

Equation 1.1 – Equilibrium reaction between water and CO₂ with carbonic acid formation.⁵²



Carbonic acid is unstable and a weak acid that acts as a catalyst of the reaction of biomass hydrolysis. Its formation causes the decrease of the pH of aqueous solution to a favourable value for the biomass hydrolysis.⁵² The increase of pressure decreases the pH and the increase of temperature increases it, (due to the lower solubility of CO₂ in water),⁵³ it is possible, by controlling the pressure and temperature conditions, to adjust the effectiveness of carbonated water as solvent for biomass depolymerization.⁵²

1.5. Enzymatic hydrolysis

The possible alternative solution for the petroleum-based liquid fuels is the production of bioethanol from lignocellulosic biomass.⁵⁴ There are two main routes to accomplish bioethanol production, either enzymatically or chemically employing acids.^{55,56} The current pathway for ethanol conversion includes an enzymatic hydrolysis step which is described as a heterogeneous reaction system in which enzymes in an aqueous environment react with the insoluble, macroscopic and structured cellulose, containing highly and less ordered regions.⁵⁷ This reaction provides the depolymerisation of the cellulose structure into its monomer sugars.⁵⁸ The enzyme based route has environmentally benefits over the chemical one, since uses moderate and non-corrosive conditions such as lower reaction temperatures (50°C), pH between 4.5 and 5, biodegradable and non-toxic reagents and produces higher conversion yields.^{56,59}

To achieve an efficient hydrolysis of cellulose the concerted action of three enzymes (cellulases) is required.¹⁶ Endoglucanases initiate the hydrolysis by randomly cleaving intermonomer bonds (β -1-4 linkages) to create free chain ends. Exoglucanases or cellobiohydrolases reacts with the free chain ends producing cellobiose, a disaccharide of glucose, which is further digested by β -glucosidase to glucose monomers.^{19,59} The rate-limiting step is defined by endoglucanases and their ability to reach amorphous regions within the crystalline structure and to create new chain ends to attack by exoglucanases.^{16,60} Figure 1.9. shows an action of each enzyme as explained above.

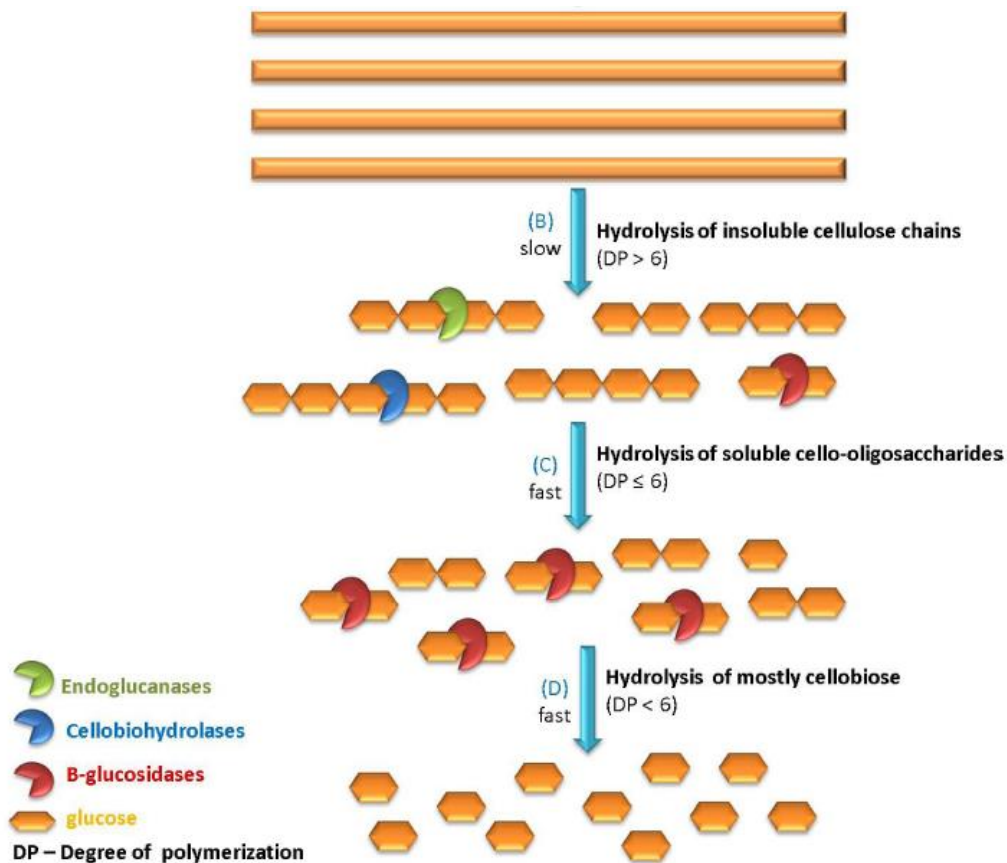


Figure 1.9 – Cellulose depolymerization by cellulases.⁵⁷

Several factors in enzymatic hydrolysis must be taken into account due to their impact on yield. A substrate concentration in the slurry solution may cause inhibition when present at high concentrations, lowers a rate of hydrolysis and also leads to difficulties in mixing and mass transfer in the solution. The resulting products from the hydrolysis of cellulose are glucose and cellobiose, which causes inhibition of the cellulase, lowering its activity. High enzyme substrate ratio, to a certain level, increases hydrolysis yield and rate, generating, however, high costs because of high enzyme requirements. Pre-treatment applied, temperature, pH, mixing and residence time are also factors that must be restrictedly controlled.⁶¹

Incubation times are also a concern because a long residence times lead to the deactivation of enzymes due to the formation of inhibitory products/contaminants.^{61,59} Furthermore, the irreversible adsorptions of cellulases to non-polysaccharides components of the biomass also cause lower enzyme activity.⁵⁹

2. Objectives

The objective of this work was to study the effect of high pressure CO₂-H₂O technology on the deconstruction of the lignocellulosic structure of wheat straw with the purpose of maximising the valorisation of this raw material. The wheat straw valorisation routes chosen to be studied in the present work were the xylo-oligosaccharides production from the hemicellulose fraction and the conversion of cellulose to easily transformable sugars (glucose) for potential posterior valorisation. Thus, the effect of high pressure CO₂-H₂O technology in both liquid and solid fractions produced was examined.

3. Materials and Methods

3.1. Materials

Wheat straw provided by, INIAV, I.P. – Estação Nacional de Melhoramento de Plantas (Elvas, Portugal), was milled to a particle size smaller than 1.5mm using a laboratory mill (IKA® WERKE, MF 10 basic, Germany). The milled straw, with an 8% w·w⁻¹ moisture calculated, was stored at room temperature for further use.

The carbon dioxide used was purchased from Air Liquide, AlphaGaz™ gamma, Paris, France with ≥99.99% w·w⁻¹ purity.

For chemical analyses it was used an aqueous solution of sulfuric acid 72% (w·w⁻¹) prepared from a 96% (w·w⁻¹) solution supplied by Panreac Química, Barcelona, Spain. For the recovery of the gas phase an ethanol solution (96% v·v⁻¹) acquired from Carlo Erba Group, Arese, Italy was used.

All FT-IR samples were prepared with KBr (≥99.5 trace metal basis) purchased from Sigma-Aldrich Co. (St. Louis, MO, USA).

For the enzymatic hydrolysis sodium citrate buffer 0.1M at pH 4.8 was prepared using citric acid monohydrate (99.7% v·v⁻¹ purity) bough from VWR International Ltd. – Leicester, England. Sodium azide (99% v·v⁻¹ purity) bough from Merck – Darmstadt, Germany, was used to prepare 2% aqueous solution of sodium azide. NaOH and distilled water were also used. Commercial enzymatic preparations of cellulases (Celluclast 1.5L) and β-glucosidases (Novozyme 188) with 105.89 FPU·mL⁻¹ and 798.56 FPU·mL⁻¹ respectively were bought from Novozymes – Bagsvaerd, Denmark.

For the phenolics compounds quantification gallic acid (99% v·v⁻¹ purity) acquired from Panreac, Quimica SA was used to prepare a gallic acid 0.6 g·L⁻¹ solution. Sodium carbonate 7.5% (w·v⁻¹) was prepared from the reagent sodium carbonate (99% v·v⁻¹ purity) from Riedel-de Haen and Folin-Cicalteu reagent bought from E. Merck, Darmstasdt, was used to prepare a 1·10⁻¹ (v·v⁻¹) Folin Cicalteus' solution.

3.2. High pressure CO₂-H₂O pre-treatment of wheat straw

The high pressure H₂O-CO₂ pre-treatment was performed in a stainless steel reactor of 600mL (series 4560, Parr Instruments Company, Moline, Illinois, USA) at various pressures (0, 15, 30, 45 and 54 bar) temperatures (35, 130, 215 and 225°C) and periods of time (0, 30, 60, 90, and 180min) chosen according to literature data.^{40,62} The reactor was loaded with straw and water, with a liquid-solid ratio of 10 (150 g of H₂O·15 g dry wheat straw⁻¹ and 100 g of H₂O·10 g dry wheat straw⁻¹), and then closed and pressurised until the desired initial pressure was reached. When the final temperature was attained, the reactor was rapidly cooled down to stop the reaction. In assays including length of time, when the desired temperature was reached, it was maintained through the period of time intended. All assays were performed with agitation of 70 rpm. Slow depressurisation of the reactor

started when the temperature dropped down until 20°C. During depressurisation, the gas phase passed through a flask, with known amount of ethanol solution (96% v.v⁻¹) acquired from Carlo Erba Group, Arese, Italy, that was kept in the ice. This procedure allowed the dissolution of volatile compounds present in the gas phase. The resulting product (liquor and solids) of these reactions was pressed and then the liquor was vacuum-filtered using paper filters (Ø = 150 mm, no. 1235 and 1242) from Filter-Lab, Microchip Technology Inc., Arizona, USA. In Figure 3.1 is presented a scheme of the apparatus used.⁶²

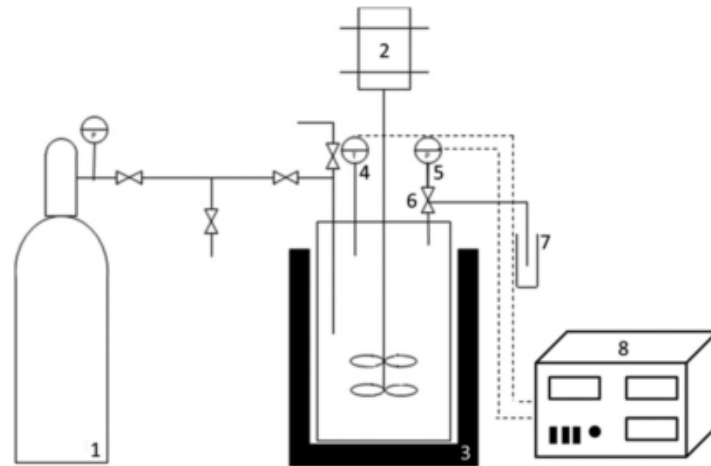


Figure 3.1 – Scheme of the high pressure CO₂-H₂O pre-treatment apparatus. 1 – CO₂ cylinder; 2 – Magnetic drive; 3 – Heating mantle; 4 – Thermo par; 5 – Pressure transducer; 6 – Depressurisation valve; 7 – Vial filled with ethanol; 8 – Pressure and temperature PID controller.

To analyse the obtained results the combined severity factor (CS_{pCO_2}) was determined using the following equation:

Equation 3.1

$$CS_{pCO_2} = \log(R_0) - pH$$

Where,

Equation 3.2

$$\log(R_0) = t \cdot e^{\left(\frac{T-100}{14.75}\right)}$$

Where t is the reaction time in minutes, T the final temperature in °C and 14.75 an empirical parameter related with activation energy and temperature.

and

Equation 3.3

$$pH = 8.00 \times 10^{-6} \times T^2 + 0.00209 \times T - 0.216 \times \ln(p_{CO_2}) + 3.92$$

Where p_{CO_2} is the partial pressure of CO₂ expressed in atmospheres.⁶³ Determination of p_{CO_2} is showed on annex A.

In order to study the effect of CO₂ concentration in severity conditions, CO₂ density was calculated through Peng-Robinson equation of state (PR-EOS) using the initial CO₂ pressure and temperature for each pre-treatment:

Equation 3.4 – Peng-Robinson equation of state (PR-EOS)

$$p = \frac{RT\rho}{(1 - b\rho)} - \frac{a\rho^2}{1 + 2b\rho - b^2\rho^2}$$

Where, $a = a_c\alpha$;

$$a_c = 0.45723553 \frac{R^2 T_c^2}{p_c}$$

$$\alpha = [1 + \kappa(1 - \sqrt{T_r})]^2;$$

$$\kappa = 0.37464 + 1.54226\omega - 0.26993\omega^2.$$

$$T_r = \frac{T}{T_c}$$

The constants used are: T_c (CO₂)= 304.2 K; p_c (CO₂)= 73.8 bar; ω (acentric factor)= 0.228; R (gas constant)= 8.314x10⁻² L·bar·K⁻¹·mol⁻¹.

The data used to determine CO₂ density and number of moles of CO₂ in the reactor at each reaction condition is present in annex B.

3.3. Chemical analyses

3.3.1. Solids moisture determination

For each solid sample, two nickel plates were placed in the 100°C stove for at least 5h to remove their humidity. Around 0.7 grams of sample was weighted in each plate and then placed in the 100°C stove for at least 18h, after which were weighted.

3.3.2. Liquors dry weight determination

For each liquid sample, two nickel plates were placed in the 100°C stove for at least 5h to remove their humidity. 5 mL of sample was weighted in each plate and then placed in the 100°C stove for at least 18h, after which were weighted.

3.3.3. Characterisation of the feedstock material composition

The feedstock was milled to a particle size smaller than 0.5 μm and the moisture content was determined as described in 3.3.1. section.

In the first step of acid hydrolysis, the milled straw are subjected to 1 h in a water bath set at 30°C with 72% w·w⁻¹ H₂SO₄. In the second step, the mixture was diluted to 4% w·w⁻¹ H₂SO₄ with distilled water (18.2 MΩ·cm⁻¹) produced by the PURELAB Classic Elga system and placed in the autoclave (Uniclave, Portugal) for 1 hour at 121°C. The content in sugars (glucose, xylose and arabinose) and

acetic acid was quantitatively and qualitatively determined through an Agilent 1100 series HPLC system, Santa Clara, CA, USA, equipped with refractive index detector and a Biorad Aminex HPX-87H column (Hercules, CA, USA). The set conditions of the column were: 50°C, 0.4 mL·min⁻¹ flow rate with 5 mM H₂SO₄. Before running in HPLC, all samples were filtered with syringe filters (0.22 µm) from Whatman, GE Healthcare Life Generations, Buckinghamshire, United Kingdom. The acid insoluble residue was considered as Klason lignin with correction for acid insoluble ash which was determined by subjecting the acid insoluble residue in the muffle at 550°C for 5 hours. After HPLC analysis the %Gn, %Xn, %Arn, %LK and %GAc were determined as explained in annex C.

Protein quantification was performed by the Kjeldahl method using the Nx6.25 conversion factor.

The crucible previously dried and tared porcelain with dry sample (1 g) was burned on a hotplate. Next were placed in muffle furnace (Heraeus D-6450, Germany) at 550 ± 5°C for a period of not less than 5 hours. After this time, cooled to room temperature in a desiccator and were weighed on an analytical balance. The value obtained is the amount of ash present in the sample. This procedure was repeated at least in duplicate.

3.3.4.Characterisation of the processed solids

The solid phase resultant from the reaction was washed with ultra-pure water and oven-dried at 45°C for at least 48h. Afterwards the solids were exposed to room conditions for 48h and then subjected to the same procedure as already described for feedstock material.

3.3.5.Liquor and post-hydrolysate characterisation

The liquid phase (liquor) resultant from the reaction was filtered with 0.22 µm pore filter and then analysed through HPLC with a flow rate of 0.6mL·min⁻¹. The content in sugars (glucose, xylose, arabinose) and acids (acetic, formic and levulinic) was revealed with a refractive index detector and furfural and HMF with an UV/Vis detector at 280 nm.

For the determination of total sugar content of the liquor, a determined amount of sample was subjected to an acid hydrolysis with a 4% (w·w⁻¹) H₂SO₄ for 1h at 121°C in an autoclave (Uniclave, Portugal)⁶⁴. This procedure resulted in the conversion of oligosaccharides in their monomeric units which are quantified by HPLC, as well as acids and furfural and HMF.

3.4. Gas phase

The depressurised gas phase was analysed by HPLC with an UV/Vis detector at 280 nm to examine the presence of volatile degradation compounds, namely furfural and acetic acid.

3.5. FT-IR measurement of cellulose crystallinity

The influence of high-pressure CO₂-H₂O treatment on cellulose crystallinity was evaluated in treated (autohydrolysis and high-pressure CO₂-H₂O at 225°C and non-treated samples. About 1.8 mg of

sample was milled together with 50 mg of KBr during 10 minutes with the goal of reaching a homogeneous appearance. Then the mixture was pressed with 8.5 tonnes for 5 minutes. The same procedure was made for all tree samples.

Fourier transform infrared spectroscopy (FT-IR) was performed using FT-IR spectrometer Spectrum BX, Perkin Elmer, Inc. (San Jose, CA, USA), equipped with a DTGS detector and KBr beam splitter. The operating system used was Spectrum software (Version 5.3.1, Perkin Elmer, Inc., San Jose, CA, USA). FT-IR spectra were acquired at 4000-400 cm^{-1} with a resolution of 4 cm^{-1} . The lateral order index, LOI, $(A_{1437\text{cm}^{-1}}/A_{898\text{cm}^{-1}})^{65}$ was calculated using total height.

3.6. SEM analysis

Scanning electron microscopy (SEM) was used to monitor the changes in morphology before and after $\text{CO}_2\text{-H}_2\text{O}$ high pressure pre-treatment. A XL30 FEG Philips scanning electron microscope operated at 15 keV was used to image the samples. Prior to imaging, the samples were sputter-coated with gold-palladium in an EMITECH k575x to make the fibers conductive. The parameters of sputter current and time were set to 100 mA and 30 seconds in an inert atmosphere with argon and hydrogen. Prior to coating, solid samples were clean under vacuum.

3.7. Enzymatic hydrolysis

Determination of moisture of each sample was made prior to weighting the wheat straw samples. Then it was weighted 1.5 g in an oven-dry basis of each sample and added to 2 flasks. 5 mL of 0.1 M sodium citrate buffer (pH 4.8) and 0.1 mL of 2% sodium azide solution, to prevent growth of microorganisms during digestion, were added to the flasks. The Celluclast 1.5L and Novozyme 188 activities are 105.89 $\text{FPU}\cdot\text{g}^{-1}$ and 798.56 $\text{pNPGU}\cdot\text{g}^{-1}$ cellulose, respectively. The volumes of enzyme solutions to be added to each test flask is determined by their activity.

Recommended by NREL protocol loads of Celluclast 1.5L and Novozyme 188 are 60 $\text{FPU}\cdot\text{g}^{-1}$ and 64 $\text{pNPGU}\cdot\text{g}^{-1}$ of cellulose, respectively. It is assumed that in 0.15 g of lignocellulosic test specimen there is an amount of 0.1 g of cellulose, thus, the load of enzymes to be added will be 6 FPU for Celluclast and 6.4 pNPGU for Novozyme. It was concluded that 56 μL and 8 μL of Celluclast 1.5L and Novozyme 188, respectively, were the amounts to add to each flask. Then the volume to add of distilled water was determined so that the total volume on the flask was 10 mL. In the third flask were added the same reagents as in the previous except for the enzymes.

It was also prepared in a flask a blank for enzymes which contained the buffer citrate and sodium azide solutions, water and enzymes. No lignocellulosic materials were added to this fourth flask.

All the flasks were tightly closed and placed in a rotation incubator, Optic Ivymen® System (Spain), at 50°C for 96h under 250 rpm. Samples from each flask were collected in 6h, 24h, 48h, 72h and 96h to eppendorf's and placed in an 90°C water bath for 5 minutes to deactivate the enzymes. Then samples were allowed to cool for posterior filtration with 13 mm diameter and 0.22 μm disposable nylon filters.

3.7.1.Characterisation of the samples composition

Sugars (glucose, arabinose and xylose) from all collected samples were analysed by HPLC using the refractive index detector with a $0.6 \text{ mL}\cdot\text{min}^{-1}$ flow rate. The content in these sugars was determined by the construction of calibration curves with sugar solutions with known concentrations.

After HPLC analysis the glucose digestibility was determined as shown in annex D.

3.8. Quantification of total phenolics

Quantification of total phenolic compounds was done through the Folin-Cicalteu method. Gallic acid $0.6 \text{ g}\cdot\text{L}^{-1}$, sodium carbonate $7.5\% \text{ (w}\cdot\text{v}^{-1})$ and Folin-Cicalteu $1/10 \text{ (v}\cdot\text{v}^{-1})$ solutions were prepared and $2\mu\text{L}$ of the samples to be quantified was filtered with $0.22 \mu\text{m}$ filters and diluted with Mili-Q water using 1:10 and 2:10 dilution factors.

It was added to a test-tube with lid, properly identified, $100 \mu\text{L}$ of sample, 4 mL of Folin-Ciocalteu solution $1/10 \text{ (v}\cdot\text{v}^{-1})$ and 4 mL of sodium carbonate $7.5\% \text{ (w}\cdot\text{v}^{-1})$ and after each addition it was stirred on vortex. All the tubes were incubated in a bath at $45 \text{ }^\circ\text{C}$ for 15 minutes. In the end each solution was stirred and the absorbance was measured at 765 nm . This procedure was done in triplicate in order to minimize dilution associated error.

Calibration curve was constructed in the same manner with different gallic acid concentrations (0; 0.06; 0.15; 0.30; 0.45; 0.54; $0.60 \text{ mg}\cdot\text{mL}^{-1}$).

The results are expressed in gallic acid equivalent (GAE) $\text{mg}\cdot\text{mL}^{-1}$ of samples' solution by comparison with the GAE pattern curve (see annex E).

4. Results and Discussion

4.1. Chemical composition of wheat straw

The composition of untreated wheat straw was determined and is presented in Table 4.1. As it can be seen, total content in polysaccharides is 64%, among which 38.8% is cellulose, in a form of glucan and 25.2% is hemicellulose which is the sum of xylan, arabinan and acetyl groups. Characterisation of wheat straw is in good agreement with the results of the compositional analysis obtained from Carvalho et al.⁴⁰ and Magalhães da Silva et al.⁶²

Table 4.1 – Macromolecular composition of wheat straw (% of dry weight)

Component	This work ^a	Carvalho et al. ⁴⁰	Magalhães da Silva et al. ⁶²
Cellulose ^b	38.8±0.1	38.9±0.2	38.5±0.1
Hemicellulose	25.2	23.5	24.9
Xylan	19.5±0.4	18.1±0.3	19.1±0.6
Arabinan	2.9±0.01	3.0±0.2	3.0±0.1
Acetyl groups	2.7±0.03	2.5±0.1	2.7±0.2
Klason lignin	17.6±0.1	18.0±0.5	17.7±0.1
Protein	4.7±0.1	4.5±0.5	4.7±0.1
Ash	10.7±0.1	9.70±0.03	10.7±0.1
Others ^c	3.0	5.5	3.5

^a Average of two replicates; ^b Measured as glucan; ^c Measured by difference

4.2. High-pressure CO₂-H₂O

4.2.1. Effect of reaction severity on pre-hydrolysate composition

A series of hydrolysis experiments have been carried out under variable conditions such as reaction temperature (130, 215 and 225°C), initial pressure of CO₂ (0, 15, 30, 45 and 54 bar) at non-isothermal conditions in order to assess the efficiency and selectivity on xylan conversion to xylo-oligosaccharides (XOS). A 10:100 and 15:150 (w·w⁻¹) biomass/water ratio was also examined. The CS_{pCO₂} was applied with the objective to encompass all these variables and to facilitate the

comparison of the obtained data. The determination of the combined severity factor has into account the time that the system takes to be heated until the desired temperature, which in turn depends on the water/biomass loading and the final temperature. Also the pH in the medium reaction contributes to the severity factor value and this parameter depends on the partial pressure of CO₂ in the system.

Both, high-pressure CO₂-H₂O and water-only reaction (autohydrolysis) resulted in liquors containing a mixture of hemicellulose constituents such as xylose and arabinose namely in oligomer form, acetic acid and furfural (the main decomposition product of pentoses) and glucose as oligosaccharide obtained from cellulose.

As it is shown in Table 4.2 and Table 4.3 presented below, XOS is the main compound present in liquors produced in all experiments. The amount of XOS recovered was highly dependent on the reaction conditions. When wheat straw was pre-treated at $CS_{pCO_2} = -0.33$, xylan to XOS yield of 61.7% was obtained and it corresponds to concentration of XOS as high as 11.4 g·L⁻¹. Under this condition a high quality liquor, rich in pentose sugars with low amount of degradation products (1.7 g·100 g⁻¹), was obtained. At $CS_{pCO_2} = 0.19$, a decrease of XOS concentration and yield to the lowest value of 4.1 g·L⁻¹ found in all experiments was detected. At this condition, an extended xylan hydrolysis (24.2% of xylose and 12.8% of furfural) coupled with the loss of XOS yield (64% lower in comparison with the best XOS yield condition) was observed. Additionally, interesting is that comparing the XOS yield at CO₂-H₂O processing at $CS_{pCO_2} = -0.33$ with the autohydrolysis $CS_{pCO_2} = 0.02$, a 45% higher XOS yield was produced in CO₂ coupled treatment. It may indicate that presence of CO₂ helps to promote the hydrolysis of hemicellulose xylan to XOS. For reactions performed at 130°C independently of CO₂ pressure used the concentration of XOS is quite low (from 1.3 to 1.5 g·L⁻¹).

Xylose is the main monosaccharide present in the liquor followed by the second monosaccharide - arabinose. Under the best XOS yield condition, the concentration of released xylose and arabinose corresponds to 15% and 46.5% of initial xylan and arabinan contents, respectively. The concentration of xylose increased with the severity of the reaction up to $CS_{pCO_2} = 0.11$, for which a maximum concentration of 5.3 g·L⁻¹ was obtained. At the harshest conditions ($CS_{pCO_2} = 0.19$), the xylose concentration starts to decrease caused by its degradation giving furfural with 1.7 g·L⁻¹ concentration. In all other reactions, with less severe conditions, furfural was formed almost in negligible amounts as depicted in Table 4.3.

Gluco-oligosaccharides (GlcOS) and glucose follows similar pattern to XOS and xylose. A concentration of GlcOS tends to decrease and monomers of glucose concentration increases with reaction severity. The formation of GlcOS might have an origin in the effect of the reaction conditions on cellulose, especially on the amorphous one which is more susceptible for hydrolysis even at mild conditions. To confirm this concept, the crystallinity index from FT-IR measurements was calculated (it is shown in section 4.2.5). The FT-IR results confirm that autohydrolysis is a less severe process and that GlcOS is mostly formed from amorphous cellulose. In case of CO₂ coupled process the amorphous cellulose is hydrolysed at a larger extent than in autohydrolysis and crystalline cellulose is also affected allowing a progressive hydrolysis of cellulose. The liquor obtained in the studied

processes contained acetic acid in both forms: as free acetic acid and as acetyl groups bounded to OS (AcOS). As expected the maximum acetic acid ($4.0 \text{ g}\cdot\text{L}^{-1}$) was achieved at the severest condition while the highest AcOS concentration was obtained at moderate $CS_{\text{pCO}_2} = -0.33$. The mechanism of this process is analogous to previously discussed conversion of XOS to xylose. More severe conditions favour hydrolysis of AcOS to acetic acid therefore the concentration of acetic acid increases with the increase of severity factor. King and co-workers obtained similar results for experiments based on hydrolysis of switchgrass with carbonated water to produce carbochemicals in the range of temperature from 220 to 310°C and commensurate higher pressure (68 bar) in a semi-continuous batch flow system. The aliphatic acids (acetic and formic) were produced at levels of 3-6 $\text{g}\cdot 100\text{g}^{-1}$ of feedstock while furfural was rapidly produced at 310°C within 10 min.⁶⁶ The examined conditions allowed to produce liquors rich in oligosaccharides in a total concentration of $18.6 \text{ g}\cdot\text{L}^{-1}$ at $CS_{\text{pCO}_2} = -0.33$. The produced solution was mostly constituted by XOS which is a major product among oligosaccharides present, corresponding to 61% of them.

Comparison between XOS concentrations obtained at 130°C and 225°C conditions shows the important effect of temperature on hydrolysis of biomass. For instance, at 30 bar, it was observed an increase more than 500% for increase of temperatures from 130°C to 225°C. Although dissolution of CO_2 in water increases with an increase of CO_2 pressure and reduces with increases of temperature, XOS content shows only a 9% increase associated to the increase of CO_2 pressure by 30 bar at 130°C, while at 225°C, an analogous pressure increase gives an increase of 24% of XOS. These results also evidence the strong influence of temperature, that despite of enhancing water acidity, also increases acetic acid concentration in solution, which acts as a catalyst.

Data available for 130°C shows that the XOS average values obtained were close to $1.4 \text{ g}\cdot\text{L}^{-1}$ and the remainder constituents from the liquor are present in equally low amounts. At this temperature it was expected that hydrolysis of glycosidic linkages would be lower, when compared with 225°C, due to minor auto-ionization of water. Presence of acetic acid in liquors obtained at 130°C reactions confirms that acetyl groups are the first to be hydrolyzed, as described elsewhere.⁴⁰ For the 130°C conditions, presence of CO_2 enhances production of XOS and GlcOS. In fact, at lower temperatures dissolution of CO_2 in water increases leading to greater amounts of carbonic acid in solution, as revealed from the estimated pH. The literature reports^{67,68} illustrate that to achieve the same compound concentrations a shorter time of pre-treatment is needed when the severity increase is noted. As observed, for 130°C the increase of severity of reaction conditions by the increase of CO_2 pressure, drives to slight increase of XOS and do not promote a degradation of sugars. This may indicate that at these conditions xylan degradation kinetic is at an early stage. To better understand reaction pathway more experiments should be done with longer periods of time.

In this work, increase in CO_2 concentration was achieved either by lowering the initial temperature of the system before CO_2 pressurisation, increasing CO_2 pressure or lowering the biomass loading. For both biomass loading ($150\cdot 15^{-1}$ and $100\cdot 10^{-1}$) at constant temperature (225°C) it was observed that an increase in number of moles of CO_2 by the increase of pressure from 15 bar to 30 bar and 45 bar resulted in a decrease in XOS concentration. This decrease comes from the increasingly higher

severity of the reaction conditions guiding to liquors with higher concentrations of xylose and furfural. At $100 \cdot 10^{-1}$, the increase of pressure to 30 bar and 45 bar causes a much more accentuated reduction in XOS than for $150 \cdot 15^{-1}$.

The obtained results show that 50% of reduction in biomass loading leads to an increase of 17% of moles of CO_2 and 14% of XOS (15 bar pressure). There is consistency between results from this work and Magalhães da Silva et al. since there were also reported better results regarding XOS concentration at lower biomass loadings ($75 \cdot 7.5^{-1}$). The lowest XOS concentration obtained coincided with the highest CO_2 concentration ($CS_{\text{pCO}_2} = 0.19$), as expected, however at this conditions furfural was produced at lower concentration than at all others. On the other hand, the recovered gas phase (Figure 4.1) from this reaction showed the highest concentration of furfural, which explains the lower furfural concentration found in the liquor.

For each biomass loading, increase of number of moles of CO_2 resulted in increase of acidity of liquors during reaction, showing not only the presence of carbonic acid but also its augment in the system at higher CO_2 concentration. The reduction of biomass loading from $150 \cdot 15^{-1}$ to $100 \cdot 10^{-1}$ resulted in acidic liquors (comparing reactions with the same pressure), as expected, since increase of head space involves the addition of higher amounts of CO_2 into the reactor in order to exert the same pressure.

The phenolic compounds concentration in the liquors was also measured and is presented in Tables 4.2 and 4.3. The results show that at lower temperatures (130°C) the phenolic concentration is lower than at 215 and 225°C . At 225°C is observed a concentration 9-fold higher than at 130°C that shows a strong influence of temperature on lignin degradation.

The phenolic concentration follows the same trend as the lignin dissolution, since phenolic compounds result from the degradation of lignin polymer. At 130°C no significant changes are observed between 0, 30 and 60 bar pressure of CO_2 , however an increase of phenolic concentration is observed as the severity reaction increases.

At 225°C it is observed an increase by 41% of phenolics' concentration when comparing autohydrolysis with the CO_2 reaction at 15 bar. This demonstrates that CO_2 helps the degradation of lignin structure.

Table 4.2 – Composition of liquors ($\text{g}\cdot\text{L}^{-1}$) of each product present in the liquors ($\text{g}\cdot 100\text{ g}^{-1}$ of the initial amount present in the feedstock) obtained after high-pressure $\text{CO}_2\text{-H}_2\text{O}$ of wheat straw at 130°C .

T ($^\circ\text{C}$)	130	130	130	130	130	130
$p_{\text{CO}_2\text{initial}}$ (bar)	0	30	30	30	60	60
p_{CO_2} (bar)	1.5	43.8	43.8	43.8	114.8	114.8
$\text{CO}_2/\text{biomass}(\text{w}\cdot\text{w}^{-1})$	0.00	0.19	0.19	0.19	0.71	0.71
Log (R_0)	1.01	0.83	0.83	0.83	0.94	0.94
CS_{PCO_2}	-3.32	-2.70	-2.70	-2.70	-2.43	-2.43
pH ^a	4.33	3.56	3.56	3.56	3.38	3.38
pH ^b	5.14	5.28	5.28	5.28	5.22	5.22

Composition/yields	$\text{g}\cdot\text{L}^{-1}$	$\text{g}\cdot 100\text{g}^{-1}$	$\text{g}\cdot\text{L}^{-1}$	$\text{g}\cdot 100\text{g}^{-1}$	$\text{g}\cdot\text{L}^{-1}$	$\text{g}\cdot 100\text{g}^{-1}$
XOS	1.3	5.0	1.4	11.3	1.5	4.9
GlcOS	0.5	1.3	0.4	2.0	1.5	3.9
AcO	0.0	-	0.0	-	0.0	-
Xylose	1.1	4.9	1.5	6.7	1.7	8.1
Arabinose	0.4	12.3	0.4	11.4	0.4	13.7
Glucose	0.8	1.8	1.2	2.8	0.8	2.0
Acetic Acid	0.4	-	0.5	-	0.6	-
Furfural	0.0	0.0	0.0	0.0	0.0	0.0
HMF	0.0	0.0	0.0	0.0	0.0	0.0
Phenolics		0.83		0.85		0.95

^aestimated pH during reaction, determined using the following expression: $8 \times 10^{-6} \times T^2 + 0.00209 \times T - 0.216 \times \ln(p_{\text{CO}_2}) + 3.92$; ^bpH measured after depressurisation; XOS – Xylo-oligosaccharides; GlcOS – Gluco-oligosaccharides; AcOS – Acetyl groups linked to oligosaccharides; HMF- 5-hydroxymethylfurfural; Phenolics – phenolic compounds; - not determined

Table 4.3 – Composition of liquors (g·L⁻¹) of each product present in the liquors (g·100 g⁻¹ of the initial amount present in the feedstock) obtained after high-pressure CO₂-H₂O of wheat straw at 215°C and 225°C.

T (°C)	225	225	215	215	225	225	225	225	225	225	225	225	225	225	225	225	225	225	225	225
p _{CO2initial} (bar)	15	15	30	54	30	30	0	45	45	53										
p _{rinal} (bar)	32.6	36.4	61.0	126.3	61.9	62.1	23.6	83.7	93.0	127.4										
CO ₂ /biomass (w·w ⁻¹)	0.04	0.06	0.20	0.47	0.21	0.20	0.00	0.30	0.34	0.49										
Log (R ₀)	3.83	3.80	3.57	3.58	3.87	3.96	3.79	3.95	3.95	3.96										
CS _{P_{CO2}}	-0.48	-0.42	-0.33	-0.13	-0.09	0.00	0.02	0.08	0.11	0.19										
pH ^a	4.31	4.22	3.90	3.71	3.96	3.96	-	3.87	3.84	3.77										
pH ^b	3.97	4.14	3.87	3.80	4.03	3.78	3.77	3.74	3.68	3.55										
Composition/ yields	g·L⁻¹	g·100g⁻¹	g·L⁻¹	g·100g⁻¹	g·L⁻¹	g·100g⁻¹	g·L⁻¹	g·100g⁻¹	g·L⁻¹	g·100g⁻¹	g·L⁻¹	g·100g⁻¹	g·L⁻¹	g·100g⁻¹	g·L⁻¹	g·100g⁻¹	g·L⁻¹	g·100g⁻¹	g·L⁻¹	g·100g⁻¹
XOS	9.4	51.7	10.7	57.9	11.4	61.7	9.9	53.8	9.2	52.9	9.2	49.8	7.4	42.6	8.9	48.3	5.6	30.6	4.1	22.6
GlcOS	4.8	13.2	5.7	15.5	4.5	12.4	4.5	12.3	4.3	12.4	5.0	13.6	4.0	11.6	4.0	13.6	3.6	9.8	3.5	9.5
AcO	0.8	-	2.8	-	2.7	-	1.9	-	2.1	-	0.6	-	0.4	-	0.2	-	1.7	-	1.7	-
Xylose	2.8	13.4	3.0	14.4	3.1	15.0	4.2	20.1	3.3	16.7	4.4	21.2	3.7	18.9	3.4	21.2	5.3	25.4	5.0	24.2
Arabinose	1.2	39.5	1.2	37.5	1.4	46.5	1.3	40.8	0.8	26.5	1.2	23.5	0.8	25.7	1.1	23.5	1.0	26.4	0.8	24.4
Glucose	1.2	2.9	0.8	1.9	0.9	2.2	1.0	2.6	0.7	1.8	0.9	2.3	0.8	2.1	1.2	2.3	1.1	2.7	1.2	2.9
Acetic Acid	3.2	-	3.2	-	2.5	-	3.3	-	3.0	-	3.5	-	3.5	-	3.5	-	3.6	-	4.0	-
Furfural	0.1	1.0	0.8	6.3	0.2	1.3	0.2	1.7	0.8	6.0	1.0	7.1	1.5	12.2	1.2	7.1	0.8	6.0	1.7	12.8
HMF	0.2	0.5	0.2	0.5	0.1	0.4	0.2	0.7	0.2	0.7	0.2	0.6	0.2	0.8	0.3	0.2	0.3	0.9	0.3	1.1
Phenolics	8.66		7.27		7.17		6.73		6.30		8.13		6.15		9.18		9.76		8.20	

^aestimated pH during reaction, determined using the following expression: $8 \times 10^{-6} \times T^2 + 0.00209 \times T - 0.216 \times \ln(P_{CO_2}) + 3.92$; ^bpH measured after depressurisation; XOS – Xylo-oligosaccharides; GlcOS – Gluco-oligosaccharides; AcOS – Acetyl groups linked to oligosaccharides; HMF- 5-hydroxymethylfurfural; Phenolics – phenolic compounds; - not determined

4.2.2. Hydrolysate pH

Other important aspect examined in this work is the pH of the produced liquors. The measured and predicted⁶⁹ pH values of hydrolysates from either autohydrolysis or high-pressure CO₂-H₂O experiments are presented in Tables 4.2 and 4.3. As it can be seen, the measured pH values (after CO₂ released at room temperature) vary between 3.55 and 4.04 for experiments carried out with CO₂. The processes with CO₂ for $CS_{pCO_2} \geq 0.08$ gave pH of hydrolysate lower than this for autohydrolysis reaction (pH=3.77). Considering that no significant additional amount of acetic acid was formed during these reactions, as it is shown in Table 4.2 and 4.3, it may indicate that carbonic acid formed *in-situ* acidify the medium driving to the decrease of the final pH of the liquor. The obtained results are in contrast to those presented by van Walsum and co-workers where addition of carbonic acid increased the pH of the liquor produced.⁷⁰ These differences can be elucidated by the fact that at lower CO₂ pressure, the solubility of CO₂ in the aqueous phase is much lower (even one order of magnitude), therefore at these conditions the acidification of liquor by carbonic acid is practically negligible. For instance, for the reaction at 225°C and 15 bar of initial CO₂ pressure (32.6 bar final pressure) for $CS_{pCO_2} = -0.48$, the solubility of CO₂ in water is almost null ($x_{CO_2} = 0.0016$)⁷¹ resulting in very lower CO₂ dissolved/water ratio, which equals to 0.039. In contrast, the solubility of CO₂ in water for the harshest conditions examined ($CS_{pCO_2} = 0.19$) is $x_{CO_2} = 0.0196$ giving 0.49 g of CO₂ dissolved in water per g of biomass. This data clearly demonstrate that CO₂ pressure and by this the severity of the reaction plays an important role as at the lesser severe conditions, reactions occur in fact in the three phase system involving solid biomass, water mostly in liquid state and gaseous phase constituted almost exclusively by CO₂. Furthermore these three phase reactions give a pH of liquors similar to pH of liquor for autohydrolysis ($CS_{pCO_2} = 0.02$).

Other important aspect to be scrutinised is that at the harshest conditions, degradation products with acidic characteristic are formed, which also contribute to biomass hydrolysis and consequently guide to lower pH values of generated liquors. For example, a lower pH values were found also in hydrothermal processes reported in the literature where an extensive hydrolysis of hemicellulosic acetyl groups was found.^{72,73,74} Other very important factor influencing the pH of the liquor is the composition of biomass explored. Biomass rich in high acetyl group contents may lead to a decrease of pH during reaction. Comparison of the results obtained in this work with those reported in the literature⁷⁵ illustrates that the pH value of liquors from aspen wood pre-treatment with carbonic acid for $CS_{pCO_2} = 0.17$ is 3.95⁷⁵, and is not very different from this obtained under similar reaction conditions ($CS_{pCO_2} = 0.19$) presented in this work. On the other hand, corn stover for CS_{pCO_2} close to this got in this work gives the final pH very different (pH=4.95). According to van Walsum et al. the differences between the final pHs can be explained by the extended autocatalytic hydrolysis of acetyl groups of aspen wood in comparison with those in corn stover.⁷⁵

Although, the CO₂ experiments resulted in different pH of liquors, in fact the decrease of pH does not show significant effect on hemicellulose dissolution. For example, the difference of hemicellulose dissolution between all reactions with $CS_{pCO_2} \geq -0.13$ was only around 6%. Brunner and co-workers also found similar conclusions, where no substantial relation between hemicellulose dissolution and decrease of pH was determined.⁷⁶ Even a decrease of pH to around 2 caused by addition of sulphuric acid did not have any effect on biomass dissolution.⁷⁶

The pH of medium produced during the process and the reaction severity not only influences the liquor composition but also affects a pre-treated solid too.

4.2.3. Effect of reaction severity on gas phase composition

From the recovered gas phase, the only volatile product to be found was furfural. The concentrations of this compound present in the gas phase for each reaction are shown in Figure 4.1, presented below. Analysis of the results shows that the increase of number of moles of CO₂ increases furfural concentrations in the recovered gas phase. It can be seen that furfural is dependent not only on the number of moles of CO₂ present but also on biomass loading and temperature since a decrease in furfural with a decrease of any of these three parameters is observed. At the harshest condition ($n_{CO_2} = 9.01$ mol), the highest value of furfural equaled to 1.25 g·L⁻¹ was obtained. Since there was no furfural observed in liquors at temperature reaction of 130°C, it was also not expected its presence in the recovered gas phase.

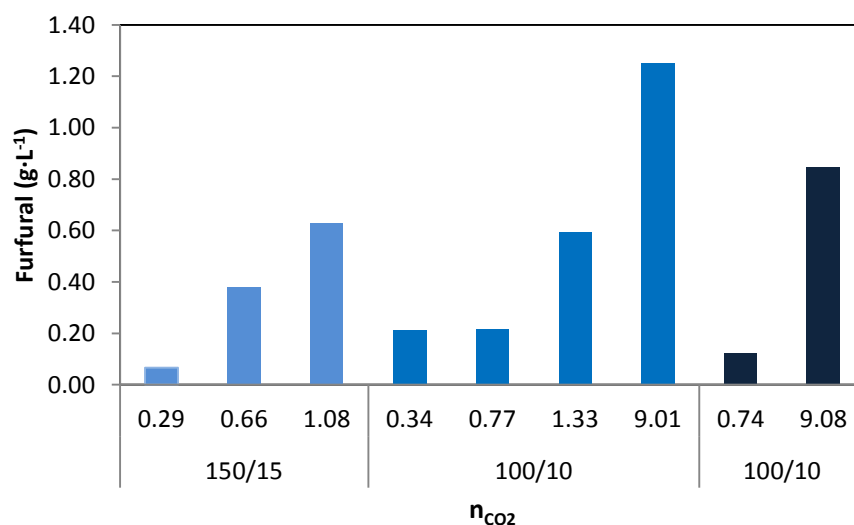


Figure 4.1 – Content in furfural (g·L⁻¹) of the recovered gas phase as a function of number of moles of CO₂. 150/15 and 100/10 represent the ratio between mass of water and mass of biomass.

4.2.4. Effect of severity on solid phase composition

Figure 4.2 summarizes the composition and yield of the pre-treated solid residues obtained either by autohydrolysis or by CO₂-H₂O under different severity conditions. For all conditions of high-pressure CO₂-H₂O processes, except for 130°C, the solid dissolution was high and superior to 50%. In comparison, the autohydrolysis reaction, similarly to CO₂-H₂O experiments, demonstrated still high solid dissolution (46.7% of initial biomass) with hemicellulose removal close to 75%. Other important aspect is that, the processed solids suffered significant changes in composition in comparison with the raw material. The degree of biomass dissolution increases almost linearly with severity factor reaching values of hemicellulose removal up to 86.4%. This demonstrates an uncompleted hydrolysis of xylan and presence of minor amount of acetyl groups as well as a complete dissolution of arabinan as its absence was determined in the processed solid. With an increase of the severity of the reaction a faster cleavage of linkages of the hemicellulose and cellulose was observed.⁷⁶ Van Walsum observed, at elevated temperatures (above 200°C), similar catalytic effect of carbonic acid on pure xylan hydrolysis allowing for an increase of pentoses release and a decrease of a degree of polymerisation of xylan oligomers in comparison with autohydrolysis (hot water).⁶⁹ The obtained data shows that cellulose, despite being partially affected by either autohydrolysis or CO₂-H₂O process, is a dominant constituent of the processed solid and its relative concentration increases with the severity of the reaction once the dissolution of hemicellulose fraction occurs. The maximum glucan content of 74.9% in the processed solid was found at CS_{pCO₂} = 0.19. The increase of severity had minor effects in glucan dissolution, with a maximum of glucan loss of 14.3% for the severest condition. The third principal component of biomass, lignin, remained in the processed solid. The recovery of lignin in solid phase was found to be between 27.0% and 31.2%. The treatments resulted in the increase of the total amounts of lignin due to lignin condensation reactions which makes even worse digestibility of the remaining cellulose fraction.^{77,78}

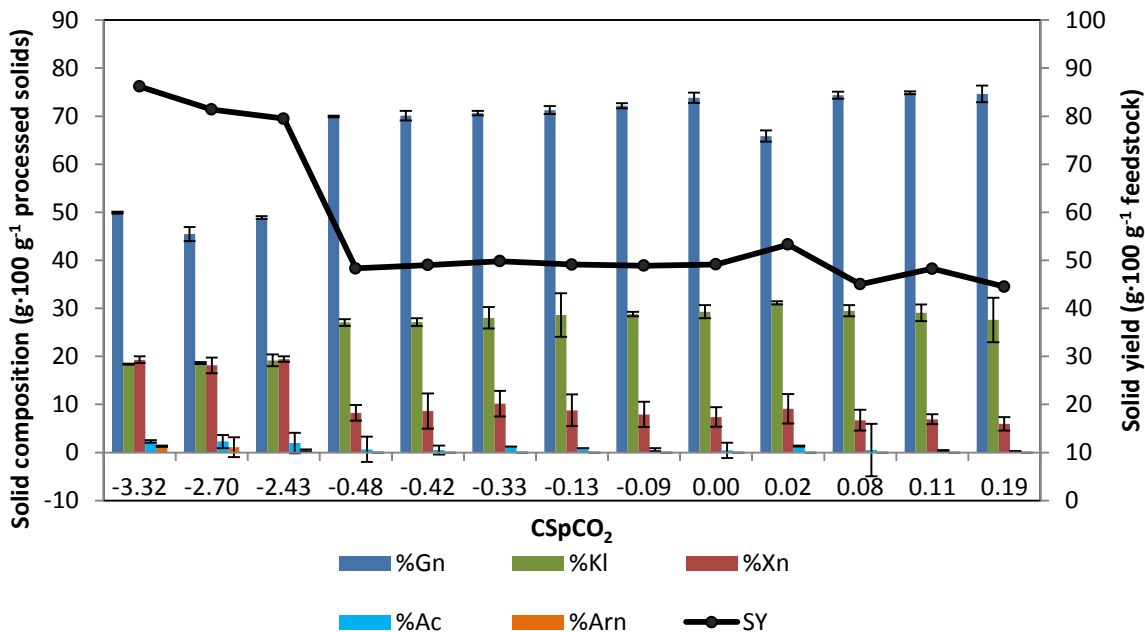


Figure 4.2 – Composition of the solids and solid yield obtained after high-pressure CO₂-H₂O

4.2.5.Characterisation of cellulose crystallinity of pre-treated solids

Fourier Transform Infrared (FT-IR) technique was selected to analyse the compositional changes regarding to cellulose crystallinity of the solid materials recovered from both autohydrolysis and high-pressure CO₂-H₂O.^{79,80,81} A LOI⁶⁵ is a tool to measure the degree of crystallinity of cellulosic material and is defined as a ratio of absorption bands at 1430 and 838 cm⁻¹. A band at 1430 cm⁻¹, assigned to a symmetric CH₂ bending vibration is “crystallinity band”, indicating that a decrease in its intensity reflects reduction in the degree of crystallinity of the samples. The FT-IR absorption band at 898 cm⁻¹, assigned to C–O–C stretching at β-(1→4)-glycosidic linkages, is an “amorphous” absorption band and an increase in its intensity happening in the amorphous samples. The results obtained for untreated, and treated by autohydrolysis (CS_{pCO₂}=0.02) and with CO₂ (CS_{pCO₂}=0.08) are given in Table 4.4 and Figure 4.3.

The analysis of the produced data shows that LOI for untreated sample is 3.28, while for autohydrolysis and CO₂ treated solids is 4.56 and 3.92, respectively. It may indicate that the untreated sample has lower crystallinity than the treated ones. However the close inspection of the obtained data shows that there is a removal of the amorphous cellulose in the treated samples, and thus a reduction of the ratio is observed when compared with the LOI of the untreated sample.

Table 4.4 – The LOI index for untreated, autohydrolysis and CO₂-treated wheat straw

	A_{898}	A_{1437}	$LOI = \frac{A_{1437}}{A_{898}}$
Untreated	0.115	0.376	3.27
Autohydrolysis ($CS_{pCO_2}=0.02$)	0.084	0.383	4.56
High-pressure CO ₂ -H ₂ O ($CS_{pCO_2}=0.08$)	0.079	0.311	3.94

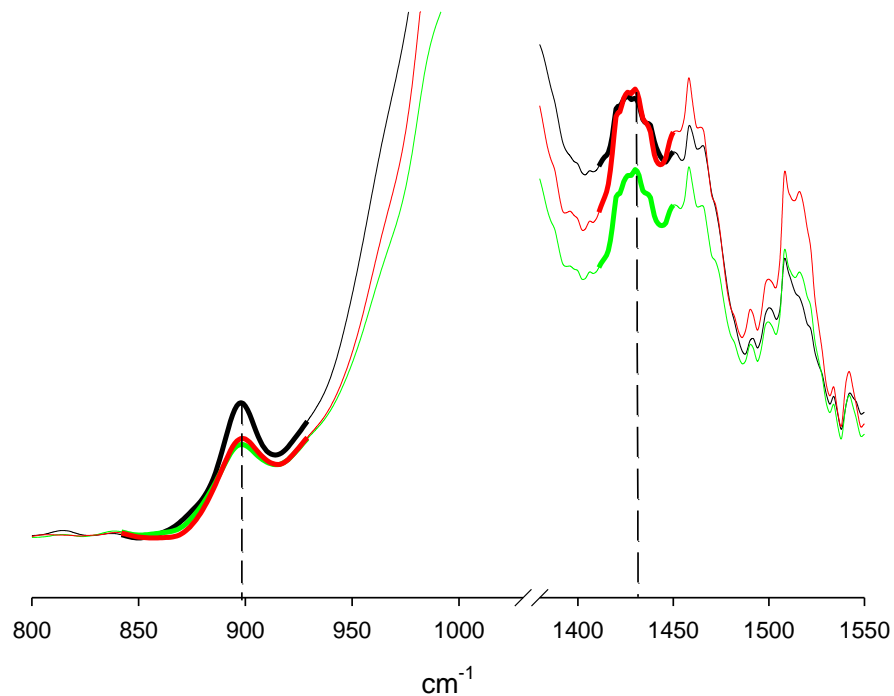


Figure 4.3 – The FT-IR spectra of untreated (black line), autohydrolysis (red line) and CO₂ processed wheat straw (green line) showing the regions for LOI determination. The adequate bands (898 and 1437 cm⁻¹) are marked by dashed lines.

The analysis of each band shows that autohydrolysis pre-treatment removes only the amorphous cellulose as the band at 898 cm⁻¹ reduced by 27% and that there is no changes in the crystalline one as the 1437 cm⁻¹ remains intact in comparison with untreated biomass. Further analysis shows that the process with CO₂ is more extensive as reduces either amorphous cellulose or crystalline one by 31% and 17%, respectively.

4.2.6. Effect of high-pressure CO₂-H₂O on morphology of wheat straw

4.2.6.1. Scanning Electron Microscopy

The aforementioned aspects are also visible on the morphology of processed solids. For the purpose of analysis of the mentioned effects the Scanning Electron Microscopy (SEM) was employed. SEM technique allowed investigating the effect of process on the ultrastructure and possible disruption of the cell walls. Figure 4.4 shows SEM analysis of native wheat straw and after either autohydrolysis (225°C) or CO₂-H₂O reactions (225°C and 45 bar of CO₂). After both pre-treatments, physical changes of raw material surface were noticeable. The grinded untreated wheat straw exhibited a rigid, tight and contiguous surface while fibres of treated samples have anomalous porosity and lamellar structures became fleecy. The treated solids are significantly more heterogeneous in structure than untreated one. This indicates that the surface of raw material was subjected to severe conditions during both processes with the dominant effect visible in case of the CO₂ involved. These morphological changes find an explanation in the previously discussed results. The extended hemicellulose removal from middle lamella caused by the reaction conditions guided to the structural changes visible. In other words, the synergetic attack of CO₂ and H₂O promotes fibre separation exposing the surface leading at the meanwhile to elevated enzymatic digestibility of the processed solid⁸² as it is also discussed below. Furthermore, the interaction between biomass with hot liquid water and high dense CO₂ lead to increase of diffusivity of gas into the biomass promoting the swelling of biomass.⁸³

Similar conclusions regarding the effect of supercritical CO₂ on physical structure of lignocellulosic materials were presented in the literature.^{84,85} Zheng et al., studied the effect of different gases such as nitrogen, helium and CO₂ and the later on has demonstrated higher glucose yields from enzymatic hydrolysis of lignocellulosic materials.⁸⁶ Narayanaswamy et al., reported that supercritical CO₂ (150°C, 241 bar, 1h and moisture of 75%) had a significant effect in opening the pores and exposing internal areas of corn stover.⁸⁴ On the other hand no effect of supercritical CO₂ on switchgrass was found probably due to rigid structure of this biomass.⁸⁴ Gao et al. discovered that reaction with supercritical CO₂ (110°C, 300 bar for 30 min and liquid/solid ratio of 1:1) promotes changes in porosity and fibers became more susceptible to enzymatic attack increasing its digestibility.⁸⁵ Contrary to the results presented in this work both referred literature studies used CO₂ explosion which has a great impact on biomass pore rupture. Presumably, rapid release of CO₂ led to explosion and the effect on pores opening is much more evident. Benazzi et al., reported that depressurisation rate of 50-200 kg·m⁻³·m⁻¹ after ultrasound assisted supercritical CO₂ pre-treatment did not result in a significant increase of glucose yield obtained by enzymatic hydrolysis. It might be explained by the slow CO₂ release in comparison to CO₂ explosion pre-treatment.⁸⁷ Ferreira-Leitão and co-workers found that the CO₂-explosion pre-treatment at 205°C for 15 min resulted in less pronounced structural modifications of the material than SO₂-explosion at 190°C for

5 min which can be directly related to the combined severity of each pre-treatment.⁸⁸ It was also observed that the SO₂-pre-treatment resulted in more extensive hemicellulose removal equals to 68.3% in comparison with 40.5% obtained from CO₂-pre-treatment. However, SO₂ is highly toxic and may present negative safety, health and environmental impacts.

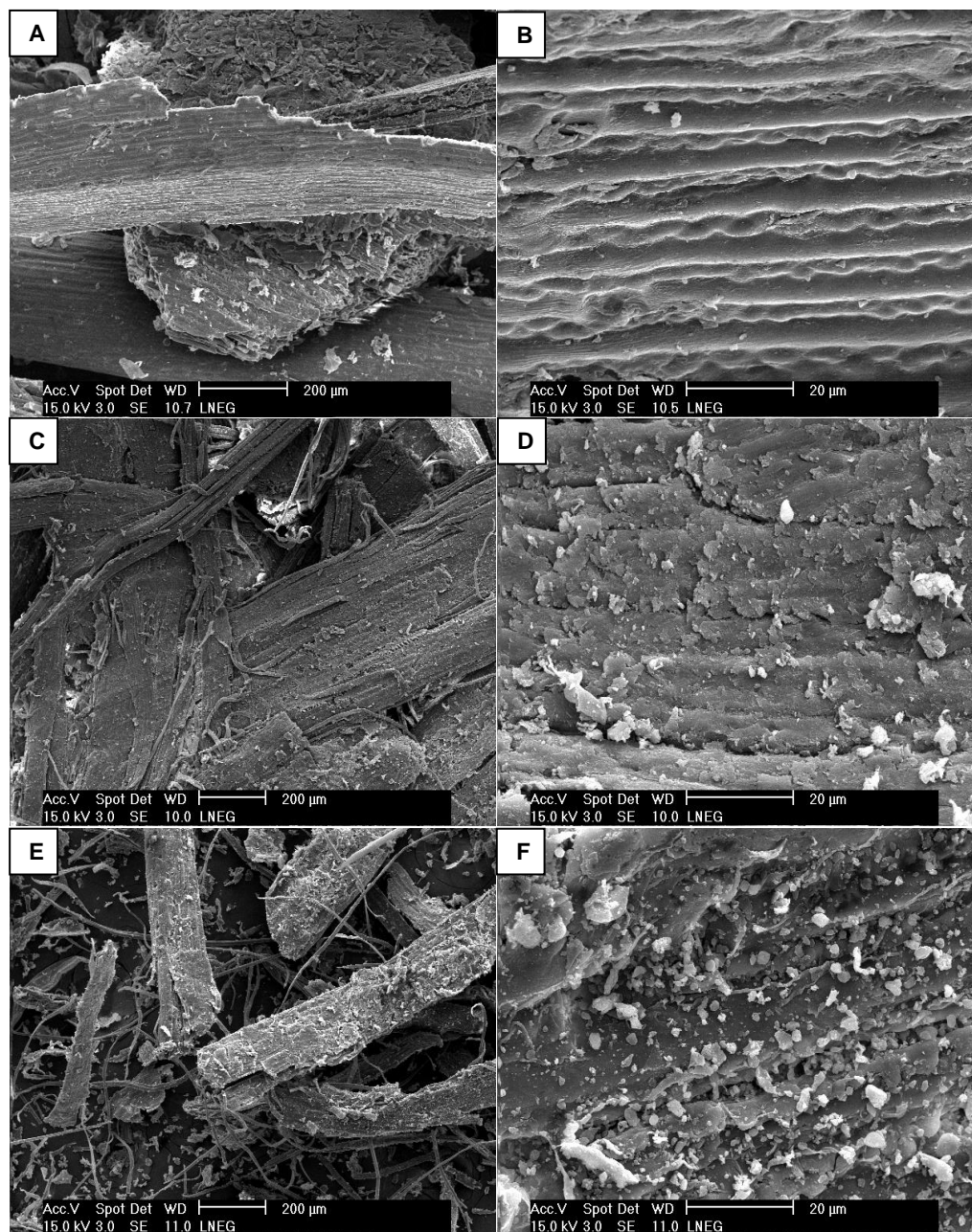


Figure 4.4 – SEM images of untreated wheat straw (A,B), autohydrolysis (C,D) and treated at 225°C with 45 bar of CO₂ (E,F). A, C and E images have an amplification of 75x and B, D and F images have an amplification of 1200x.

4.3. Enzymatic hydrolysis of pre-treated solids

To survey the influence of examined processes on the monosaccharides production from cellulose fraction, the processed solids were subject to the enzymatic hydrolysis. The enzymatic attack is affected by several factors of the pre-treatment process being essential to change the macro and micro characteristics as well as properties of lignocellulosic material making polymers such as glucan and xylan much more accessible for enzymes attack. The most important factors influencing the rate of enzymatic hydrolysis are hemicellulose and lignin content, cellulose crystallinity, degree of polymerisation²⁸ as well as liquid/solid ratio. All of these factors are strongly related with the choice of biomass processing technology and conditions employed.

4.3.1. Effect of CO₂ pressure

The wheat straw samples pre-treated at various CO₂ pressures at fixed temperature were hydrolyzed by the addition of cocktail of enzymes for 96h. Figure 4.5 shows the effect of CO₂ pressure on glucose yield from glucan for the high-pressure CO₂-H₂O reaction of wheat straw performed at constant temperature (225°C). The glucose yield increased along time of hydrolysis which indicates that enzymatic digestibility of the pre-treated solids increases. The glucose yields arise to a maximum of 56.02, 57.77, 63.93, 75.39 and 82.21% at 96 h of enzymatic hydrolysis for 0, 15, 30, 45 and 54 bar of initial CO₂ pressures, respectively.

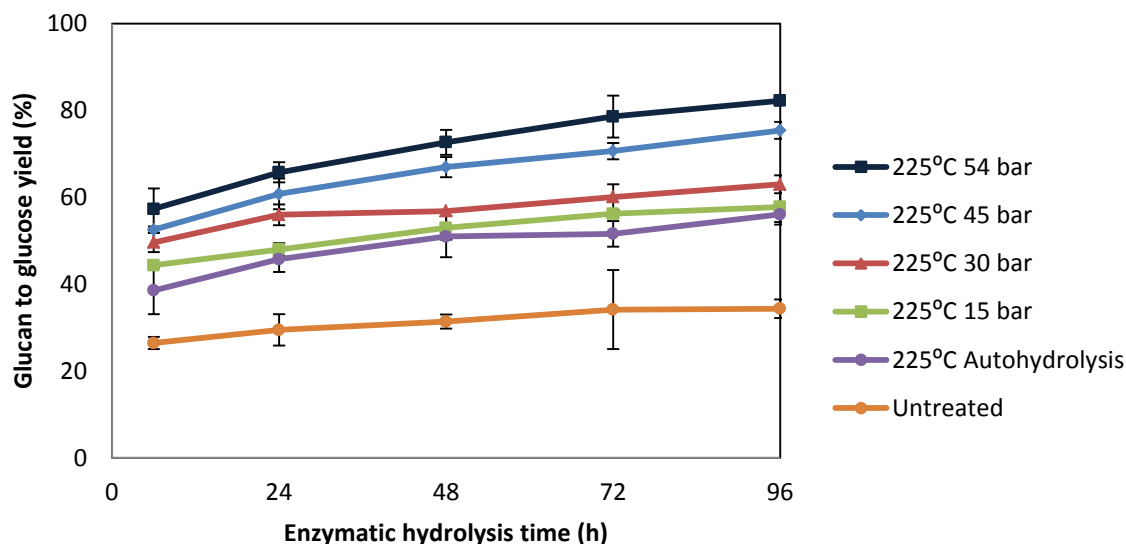


Figure 4.5 – Effect of CO₂ pressure of high-pressure CO₂-H₂O on enzymatic hydrolysis yield

The glucose yield increased by 46.8% with increasing pressure (from 0 to 54 bar of initial or from 23.6 to 127.4 bar of final pressure). It shows that CO₂ pressure plays an important role in improving the enzymatic yield. Zheng et al. studied the effect of supercritical CO₂ on hydrolysis of Avicel (commercial form of cellulose). They concluded that the disruption of cellulosic structure was

caused by CO₂ under supercritical conditions followed by quick depressurisation which increases the rate of enzymatic hydrolysis resulting in glucose yield around 50%.⁸⁹ Zheng and co-workers also investigated the effect of scCO₂ on recycled paper mix and sugarcane bagasse in which glucose yields of 75% and 22%, respectively were reported.⁸⁶ Alinia et al., found that pressure changes from 80 to 120 bar in the wheat straw pre-treatment promotes an increase of yield of reducing sugars and further increase in pressure above 120 bar does not change the final sugar yield.⁹⁰ Kim et al., studied the hydrolysis of aspen and southern yellow pine pre-treated at 214 and 276 bar of CO₂ and they did not observed any effect on enzymatic digestibility of both materials.⁹¹ The conclusion taken by Kim et al. might be burdened by presence of high lignin content in both aspen and southern yellow which may have a negative effect of enzymatic hydrolysis. It is important to mention that CO₂ not only affects the enzymatic hydrolysis under supercritical conditions but also at subcritical. For instances, sugarcane bagasse treated with 70 bar of CO₂ at 160°C for 60 min showed an increase of 36% in glucose yield in comparison with the pre-treatment without CO₂. Puri et al., studied the effect of steam and CO₂ under sub and supercritical condition on the cellulose hydrolysis of wheat straw.⁹² The maximum glucose yield of 81% was obtained at 200°C in the range of CO₂ pressure of 34.5-138 bar. Hsu et al., investigated the effect of dilute-acid hydrolysis on enzymatic hydrolysis of rice straw and a maximum sugar yield of 83% was achieved when rice straw was pre-treated with 1% (w·w⁻¹) of sulphuric acid with reaction time of 5 min at 180°C.⁹³ Also Henk and co-workers found that corn stover pre-treated with 2% (w·v⁻¹) sulphuric acid produces a cellulose digestibility higher than 80%.⁹⁴ The obtained results are in good agreement with the ones obtained in this work for 225°C and 54 bar of initial CO₂ pressure, without additional chemical catalyst. However, the spent acid and consequently neutralisation may originate gypsum which must be eliminated to make the overall process environmentally and economically feasible. Since CO₂ is easily recycled and acts as a catalyst and co-solvent, CO₂-H₂O process could be a great alternative to acid-catalysed reaction. Dilute-acid hydrolysis requires substrate washing with water and often with alkaline solution prior enzymatic hydrolysis in order to elevate the pH to the value of optimal enzyme's pH. Unlike acid-catalysed reactions, the CO₂-H₂O does not require additional water amounts and prevents the residue formation, keeping the advantages gained from employing this technology in biomass processing.

The acquired results clearly show that enzymatic hydrolysis is strongly influenced by chemical and physical effects. To investigate the effect of CO₂ on more favourable enzymatic reaction of processed solid by the removal of hydrolysis inhibitors (hemicellulose) as well as by the physical cellulose structure opening a reaction in the presence of neutral gas – nitrogen was carried out at the conditions analogous to reaction with $CS_{pCO_2} = 0.19$ (225°C and 54 bar of N₂). The processing of wheat straw with N₂ gave 9.8, 3.0 and 1.3 g·L⁻¹ of XOS, xylose and furfural respectively. At the same time the formed processed solid contained 61.2% of glucan that in the enzymatic hydrolysis process was converted to glucose giving after 72 h a 63% of glucan to glucose yield. Comparing

this data with the autohydrolysis (51.6%) and analogous with CO₂ process (78.6%) it can be concluded that presence of neutral gas which occupy the headspace of the reactor and by this creates the pressure influencing positively the biomass enhances the higher enzymatic hydrolysis. On the other hand the increase of enzymatic hydrolysis from 63% for N₂ to 78.6% for CO₂ process indicates the strong chemical effect of CO₂ on the removal of hemicellulose and by this favouring the enzymatic digestibility of glucan present in the processed solid. Figure 4.6 depicts the influence of both effects on the enzymatic hydrolysis of processed solid produced in autohydrolysis (H₂O process), N₂ (N₂-H₂O process) and CO₂ (CO₂-H₂O process).

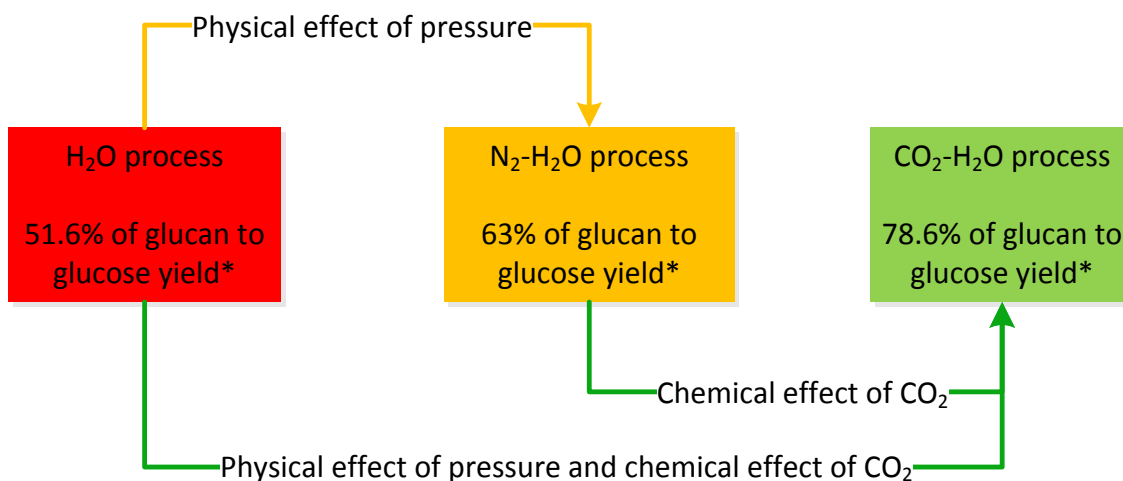


Figure 4.6 – The schematic representation of both physical and chemical effect of high pressure processes of wheat straw valorisation. *The glucan to glucose yield obtained after 72 h of hydrolysis.

4.3.2. Effect of temperature

Other possible variable influencing the hydrolysis of processed solid is temperature of process. In order to demonstrate the effect of temperature on high-pressure CO₂-H₂O, wheat straw was subject to reaction at four different temperatures (35, 130, 215 and 225°C) and fixed initial CO₂ pressure (30 bar, except for experiment at 35°C that was performed with 45 bar of initial pressure of CO₂). 215 and 225°C were temperatures examined for the hemicellulosic-sugars production while both experiments at 130°C and 35°C were carried out to demonstrate the influence of temperature on the enzymatic hydrolysis. Figure 4.7 demonstrates this relation and the maximum glucose yields for 35, 130, 215, and 225°C were 29.25, 39.97, 62.64 and 63.93%, respectively.

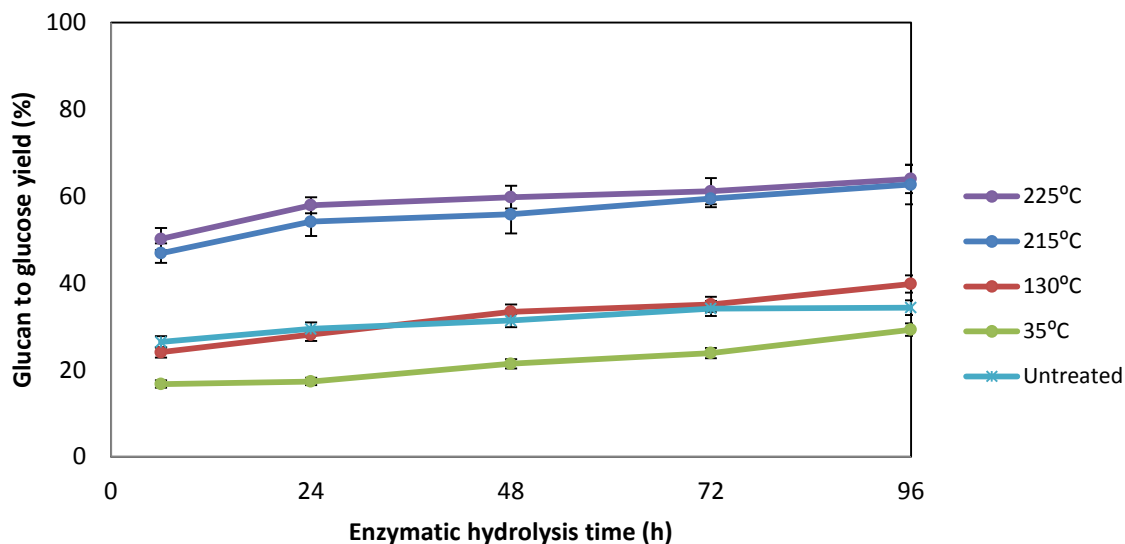


Figure 4.7 – Effect of temperature of high-pressure CO₂-H₂O on enzymatic hydrolysis.

The presented results clearly depicts that higher temperature promotes more efficient conversion of glucan to glucose. For example the increase of temperature from 130 to 215°C gives an increase of glucose yield by more than 50% (from 39.97 to 63.93%) helping produce much monosaccharide rich solution. The reaction temperature plays an important role on enzymatic hydrolysis since provides high hemicellulose removal. However, higher temperatures have the drawback of higher energy input. Other important aforementioned parameter influencing the hydrolysis of cellulose is the presence of hemicellulose and lignin. At 215 and 225°C ($CS_{pCO_2} = -0.48$ to 0.19) the composition of solid is relatively similar as demonstrated in Figure 4.2 however for 130°C ($CS_{pCO_2} = -3.32$ to -2.43) the processed solid is much richer in xylan and by this the enzymatic hydrolysis might be also affected. At 130°C, 18.14% of the mass or processed solid is xylan while in case of elevated temperature this value is much lower and equals to 10.15 and 7.93 for 215 and 225°C, respectively. This data shows the importance of reaction conditions for the hemicellulose removal. The obtained results show that process temperature of 35 and 130°C seemed to have a low impact on glucose yield. The obtained result can be explained by the low diffusivity of CO₂ at lower temperatures and thus temperature as well as CO₂ pressure is important factor in the efficient conversion of wheat straw. Kim and Hong⁹¹ tested the effect of scCO₂ at different temperatures (112–165°C). They found that at temperatures below 120°C and 214 bar for 60 min the process has no significant effect on sugar yield. However, when temperature of 160°C was used a higher glucose yield was achieved. Similar conclusions were presented by Narayanaswamy et al. who reported that the increase of temperature from 112°C to 150°C led to release of 24 and 30 g glucose per 100g of dry biomass, respectively. Gao et al. also investigated the influence of temperature of rice straw pre-treatment on glucose yield from enzymatic hydrolysis. The maximum glucose yield obtained was only 32.4% at 110°C and 300 bar of CO₂ as, according to the conclusions given, the low yield may

be caused by low temperature used in the experiments as hemicellulose and lignin start to dissolve under neutral conditions at 180°C.⁸⁵

As can be seen from Figure 4.5, the digestibilities obtained for the straw pre-treated at 35°C conditions were lower than those obtained for the untreated wheat straw. This result can be explained by the fact that during pre-treatment the amorphous cellulose is dissolved, thus the solid residue that results from it is rich in crystalline cellulose which is difficult to digest. Since no modifications has been made to the untreated wheat straw, their compositions still has both amorphous and crystalline fractions of cellulose, thus resulting in higher glucan yields. Although results for the autohydrolysis at 225°C showed that at these conditions none of the crystalline cellulose was affected by the pre-treatment, at these temperatures the morphology of the lignocellulosic structure probably is altered and thus becomes more easily hydrolysable.

4.3.3. Effect of reaction time

The effect of time on the high-pressure CO₂-H₂O at 130°C and 0, 30 and 45 bar of CO₂ was also investigated. The glucose yields for 30 min of reaction time were 40% and 42% at 130°C for 30 and 54 bar of CO₂, respectively, compared with 34% for the untreated wheat straw. The effect of time reaction is slightly more pronounced for autohydrolysis experiment, where the time applied was longer (60 minutes) than the two mentioned experiments. An improved glucose yield of 39% was obtained in comparison to untreated wheat straw. For high-pressure CO₂-H₂O, the reaction time did not show any improvement of glucose yield, probably due to the both reduced periods of time applied and low temperature conditions. These results show that time has less influence when compared with the CO₂ pressure and even lesser when comparing with temperature applied. An increase of pressure by 30 bar at 130°C reveals an improve of enzymatic hydrolysis by 12.6%, an increase in temperature, as already shown, improves the glucose yield by more than a 50%, but an increase of time (30 min) enhances glucose yield by only 5%.

Experiments at 35°C with 45 and 15 bar with periods of time of 0, 90 and 180 min were performed as well. The glucan yields obtained at these conditions are lower than those obtained for the untreated wheat straw and comparison between reactions with 0 and 180 minutes showed a glucan yield improvement in the range of 6 to 11%. Although longer reaction times have been employed in these conditions, the temperature was too low thus resulting in low severity reactions. The lower the temperature applied, the longer the period of time employed in pre-treatment should be.

Zhang et al., reported that the glucose yield for sugarcane bagasse pre-treated with scCO₂ at 160°C and 50 bar of CO₂ for 40 min was only 28.9% (g·100⁻¹ of raw material).⁹⁵

4.3.4. Effect of CO₂/dry biomass ratio

One of the most important factors that influence the effectiveness of the biomass processing with scCO₂ is the amount of both CO₂ and biomass present in the reactor. The quantity of CO₂ for a known volume of batch reactor containing biomass is great dependent on thermodynamics at the set-point pressure and temperature pre-treatment conditions. It is clear that biomass and CO₂ quantity vary together with headspace. As it is shown in Figure 4.8, the performance of enzymatic hydrolysis is affected by CO₂/biomass ratio used in the experiments. However, this increase is more pronounced for higher temperatures (215 and 225°C) than for experiments carried out at 35 and 130°C. Although, the CO₂ is more soluble in water at lower temperatures, lower reaction temperature leads to lower dissolution of hemicellulose which decreases the efficiency of enzymatic hydrolysis independently of CO₂ loaded in the reactor. The enzymatic hydrolysis was improved only in the range of 15 to 17%, at lower temperatures. At higher temperatures, the effect of CO₂/biomass loading was much more pronounced giving a maximum glucose yield of 82.21%, at 225°C.

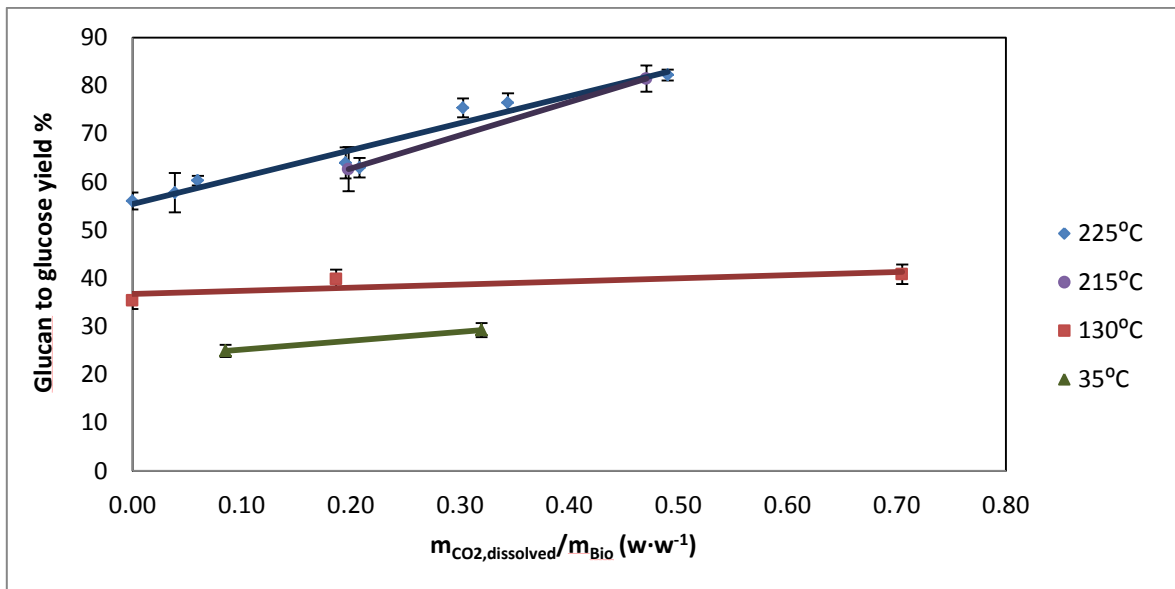


Figure 4.8 – Effect of CO₂/biomass mass ratio on glucose yield.

As experiments carry out at 225°C lead to almost total dissolution of hemicellulose, the effect of CO₂/biomass ratio in the cellulose susceptibility is much more visible on these conditions. Narayanaswamy et al., used a CO₂ to dry biomass loading ratio around 30:1 (w·w⁻¹) for scCO₂ pre-treatment where it was obtained a great glucose yield of 85% for corn stover. Also Walker and co-workers obtained the same glucose yield at the same conditions as well as at minimized ratio of 3.1:1 CO₂/biomass. Only a small quantity of CO₂ is needed to achieve “impregnation effect” of the entire biomass with CO₂ at supercritical conditions. It is important to highlight that CO₂/biomass ratio should not be considered as a single variable because it is highly influenced by reaction temperature and physical effect of CO₂.

4.4. Process overview

The valorisation of both hemicellulosic and cellulosic fractions of wheat straw polysaccharides aims to convert these inaccessible saccharides to easily transformable sugars. The integrated polysaccharide conversion to sugars in either oligomer or monomer form was analysed for all performed reactions. Figure 4.9 depicts the selected best case for high pressure CO₂-H₂O reaction.

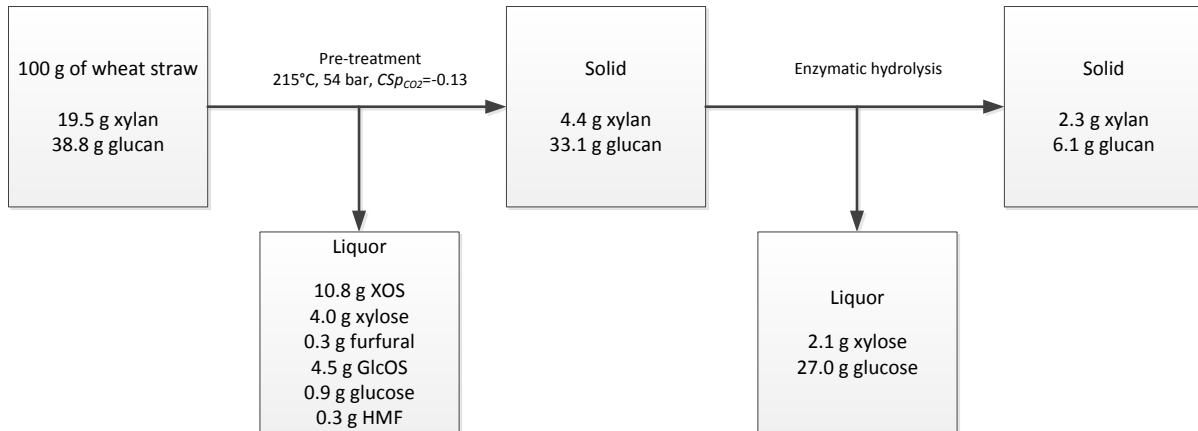


Figure 4.9 – The mass balance of integrated polysaccharide conversion.

The data for this process shows that either xylan or glucan in the integrated (pre-treatment with CO₂-H₂O and next enzymatic hydrolysis) is converted to xylose- or glucose-derived sugars with a yield of 86.3% and 83.5%, respectively. For comparison the analogous calculations for autohydrolysis process reveal yields of xylan or glucan to sugars as high as 79.6 and 61.3%, respectively. The mass balance of xylan and glucan is depicted in Figure 4.10.

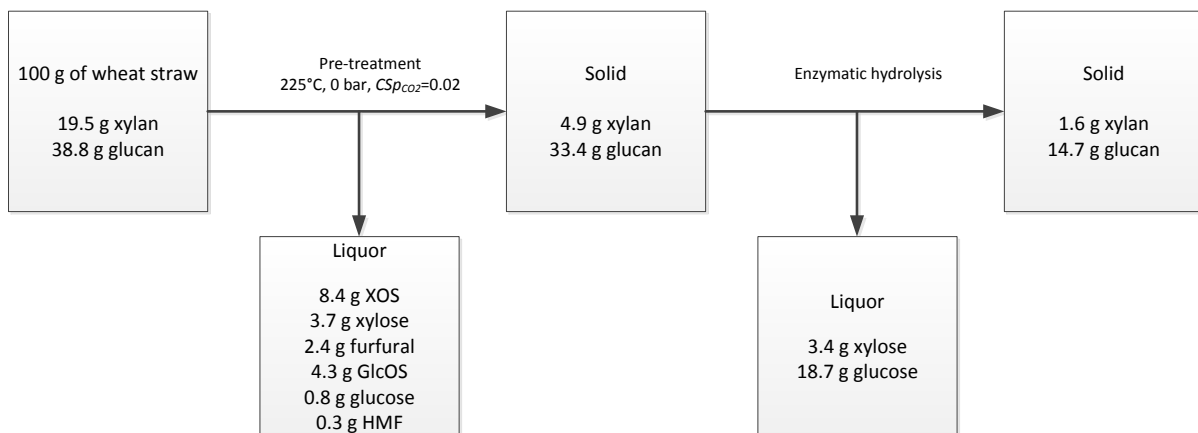


Figure 4.10 – Mass balance of xylan and glucan within the overall process for the autohydrolysis pre-treatment.

The obtained data confirms that high pressure CO₂-H₂O technology integrated with subsequent enzymatic hydrolysis of processed solid gives much higher total sugar yields (84.4%) than this for autohydrolysis only (67.4%).

5. Conclusions and Outlook

Lignocellulosic residues have the potential to become an important resource for the production of sustainable added-value products within the biorefinery concept. However, due to its complex and recalcitrant structure, a method of biomass processing is needed in order to valorize this low value feedstock. This work demonstrates a new approach for an integrated wheat straw biorefinery using a sustainable technology, high-pressure CO₂-H₂O. A CO₂ added to water-only reaction acted positively in the selective dissolution of hemicellulose resulting in an increase of 54% in xylo-oligosaccharides content at 215°C and 30 bar. This approach resulted in liquors rich in xylose oligomers (61.7%) in contrast to other valorisation methods e.g. acid hydrolysis, which produces monomers of xylose, thus it can be an advantage due to the prebiotics activities of XOS. Furthermore, XOS are one of the top value products, which production from null price bio-wastes favours the economy of the entire valorisation process of wheat straw. At milder reaction conditions (130°C), high-pressure CO₂-H₂O also enhanced XOS content, although at minor extent, revealing only an increase of 8% of these oligomers in liquors in comparison with the 54% increase at 215°C. The high-pressure CO₂-H₂O allows to carry out processes at lower temperatures in comparison with autohydrolysis, without losses of efficiency and with minimal hemicellulosic-sugar degradation. The low production of undesired degradation products coupled to high xylan dissolution yield reduces costs of downstream making this process a promising technology which can be used as a pre-treatment/hydrolysis process within a biorefinery concept. The incorporation of CO₂ into hydrothermal technologies of bio-wastes promotes higher reduction of cellulose crystallinity and physical changes on pre-treated solids superior to water-only reaction. Thus, it helps in exposing the cellulose structure to enzyme attack guiding to high quantities of fermentable sugars. After enzymatic hydrolysis assay, the effect of both reaction temperature and pressure has shown a great effect on monosaccharide yields. The maximum glucan to glucose yield of 82.21% was obtained at 225°C and 54 bar of CO₂ pressure. These yields are similar to those obtained with dilute acid hydrolysis for other lignocellulosic materials although without the use of a chemical catalyst. The integrated valorisation of polysaccharides permits to achieve an 84.7% of total sugar yield (from xylan and glucan present in the raw feedstock) in the form of mono- or oligosaccharides. The obtained results confirm that maximal exploitation of hemicellulose fraction in the form of XOS and xylose together with glucose production during the enzymatic hydrolysis are the best approaches of wheat straw polysaccharide valorisation method. Applying the methodology exploited in this work, a significant reduction of the environmental footprint of the nowadays processing technologies for this kind of feedstock can be achieved and the proposed method provides an additional economic benefits due to the high XOS production.

5.1. Perspectives

Nevertheless, to establish a solid fundament for the further application of the achieved results, it is important to examine further parameters with the objective of better understand the occurring process. Therefore, the study of different types of biomass and biomass/water ratio as well as different processing conditions (temperature, CO₂ pressure and residence time) in order to increase XOS yield and to verify the versatility of the method developed should be performed. The valorisation of other compounds present in the liquor with high economic value such as vanillin derived from lignin fraction must be investigated too. The enhanced enzymatic hydrolysis shows the potential for further improvement, which could be done by the investigation of various enzyme loadings and higher solids loadings.

6. References

1. P. Anastas and N. Eghbali. Green chemistry: principles and practice. *Chem. Soc. Rev.*, 2010, **39**, 301–312.
2. J. H. Clark, R. Luque and A. S. Matharu. Green Chemistry, Biofuels, and Biorefinery. *Annu. Rev. Chem. Biomol. Eng.*, 2012, **3**, 183–207.
3. A. R. Morais and R. Bogel-Lukasik. Green chemistry and the biorefinery concept. *Sustain. Chem. Process.*, 2013, **1**, 18.
4. J. H. Clark, F. E. I. Deswarte and T. J. Farmer. The integration of green chemistry into future biorefineries. *Society*, 2009, **3**, 72–90.
5. F. Cherubini. The biorefinery concept: Using biomass instead of oil for producing energy and chemicals. *Energy Convers. Manag.*, 2010, **51**, 1412–1421.
6. T. P. Thomsen, J. Ahrenfeldt and S. T. Thomsen. Assessment of a novel alder biorefinery concept to meet demands of economic feasibility, energy production and long term environmental sustainability. *Biomass Bioenergy*, 2013, **53**, 81–94.
7. A. Ekman, M. Campos, S. Lindahl, M. Co, P. Börjesson, E. N. Karlsson and C. Turner. Bioresource utilisation by sustainable technologies in new value-added biorefinery concepts – two case studies from food and forest industry. *J. Clean. Prod.*, 2013, **57**, 46–58.
8. S. Fernando, S. Adhikari, C. Chandrapal and N. Murali. Biorefineries: Current Status, Challenges, and Future Direction. *Energy Fuels*, 2006, **20**, 1727–1737.
9. J. H. Clark, V. Budarin, F. E. I. Deswarte, J. J. E. Hardy, F. M. Kerton, A. J. Hunt, R. Luque, D. J. Macquarrie, K. Milkowski, A. Rodriguez, O. Samuel, S. J. Tavener, R. J. White and A. J. Wilson. Green chemistry and the biorefinery: a partnership for a sustainable future. *Green Chem.*, 2006, **8**, 853–860.
10. C. V. T. Mendes, M. G. V. S. Carvalho, C. M. S. G. Baptista, J. M. S. Rocha, B. I. G. Soares and G. D. A. Sousa. Valorisation of hardwood hemicelluloses in the kraft pulping process by using an integrated biorefinery concept. *Food Bioprod. Process.*, 2009, **87**, 197–207.
11. H. Das and S. K. Singh. Useful byproducts from cellulosic wastes of agriculture and food industry--a critical appraisal. *Crit. Rev. Food Sci. Nutr.*, 2004, **44**, 77–89.
12. G. Y. S. Mtui. Recent advances in pretreatment of lignocellulosic wastes and production of value added products. *African J. Biotechnol. Vol.*, 2009, **8**, 1398–1415.
13. A. Brandt, J. Gräsvik, J. Hallett and T. Welton. Deconstruction of lignocellulosic biomass with ionic liquids. *Green Chem.*, 2013, **15**, 537–848.
14. F. M. Gírio, C. Fonseca, F. Carvalheiro, L. C. Duarte, S. Marques and R. Bogel-Lukasik. Hemicelluloses for fuel ethanol: A review. *Bioresour. Technol.*, 2010, **101**, 4775–4800.
15. D. Harris and S. DeBolt. Synthesis, regulation and utilization of lignocellulosic biomass. *Plant Biotechnol. J.*, 2010, **8**, 244–262.

16. S. Malherbe and T. Cloete. Lignocellulose biodegradation: Fundamentals and applications. *Biomass*, 2002, **1**, 105–114.
17. P. Phitsuwan, K. Sakka and K. Ratanakhanokchai. Improvement of lignocellulosic biomass in planta: A review of feedstocks, biomass recalcitrance, and strategic manipulation of ideal plants designed for ethanol production and processability. *Biomass and Bioenergy*, 2013, **58**, 390–405.
18. S. Haghghi Mood, A. Hossein Golfeshan, M. Tabatabaei, G. Salehi Jouzani, G. H. Najafi, M. Gholami and M. Ardjmand. Lignocellulosic biomass to bioethanol, a comprehensive review with a focus on pretreatment. *Renew. Sustain. Energy Rev.*, 2013, **27**, 77–93.
19. C. E. Wyman, S. R. Decker, M. E. Himmel, J. W. Brady, C. E. Skopec and L. Viikari. Polysaccharides Structural Diversity and Functional Versatility, Second Edition. *New York* 2004.
20. N. Lavoine, I. Desloges, A. Dufresne and J. Bras. Microfibrillated cellulose – Its barrier properties and applications in cellulosic materials: A review. *Carbohydr. Polym.*, 2012, **90**, 735–764.
21. Jun Xi, Wenjian Du, and Linghao Zhong (2013). Probing the Interaction Between Cellulose and Cellulase with a Nanomechanical Sensor, Cellulose - Medical, Pharmaceutical and Electronic Applications, Dr. Theo G.M. Van De Ven (Ed.), ISBN: 978-953-51-1191-7, I. .
22. M.-F. Li, Y.-M. Fan, F. Xu, R.-C. Sun and X.-L. Zhang. Cold sodium hydroxide/urea based pretreatment of bamboo for bioethanol production: Characterization of the cellulose rich fraction. *Ind. Crops Prod.*, 2010, **32**, 551–559.
23. H. A. Ruiz, D. P. Silva, D. S. Ruzene, L. F. Lima, A. A. Vicente and J. A. Teixeira. Bioethanol production from hydrothermal pretreated wheat straw by a flocculating *Saccharomyces cerevisiae* strain - Effect of process conditions. *Fuel*, 2012, **95**, 528–536.
24. Y. Zhang, A. E. Ghaly and B. Li. Physical Properties of Wheat Straw Varieties Cultivated Under Different Climatic and Soil Conditions in Three Continents. *Am. J. Eng. Appl. Sci.*, 2012, **5**, 98–106.
25. F. Talebnia, D. Karakashev and I. Angelidaki. Production of bioethanol from wheat straw: An overview on pretreatment, hydrolysis and fermentation. *Bioresour. Technol.*, 2010, **101**, 4744–4753.
26. U. K. Ghosh. Short sequence environment friendly bleaching of wheat straw pulp. *J. Sci. Ind. Res.*, 2006, **65**, 68–71.
27. Tehmina Saleem Khan and Umarah Mubeen. Wheat Straw: A Pragmatic Overview. *J. Biol. Sci.*, 2012, 673–675.
28. P. Alvira, E. Tomás-Pejó, M. Ballesteros and M. J. Negro. Pretreatment technologies for an efficient bioethanol production process based on enzymatic hydrolysis: A review. *Bioresour. Technol.*, 2010, **101**, 4851–4861.
29. A. T. W. M. Hendriks and G. Zeeman. Pretreatments to enhance the digestibility of lignocellulosic biomass. *Bioresour. Technol.*, 2009, **100**, 10–18.

30. G. Brodeur, E. Yau, K. Badal, J. Collier, K. B. Ramachandran and S. Ramakrishnan. Chemical and physicochemical pretreatment of lignocellulosic biomass: a review. *Enzyme Res.*, 2011, 17.
31. Y. Sun and J. Cheng. Hydrolysis of lignocellulosic materials for ethanol production: a review. *Bioresour. Technol.*, 2002, **83**, 1–11.
32. Fang Huang and Arthur J. Ragauskas (2013). Pretreatment techniques for biofuels and biorefineries. Berlin: Springer. p151-179.
33. V. Menon and M. Rao. Trends in bioconversion of lignocellulose: Biofuels, platform chemicals & biorefinery concept. *Prog. Energy Combust. Sci.*, 2012, 38, 522–550.
34. A. M. da Costa Lopes. Pre-treatment of lignocellulosic biomass with ionic liquids. Universidade de Aveiro, 2012.
35. A. M. da Costa Lopes, K. G. João, A. R. C. Morais, E. Bogel-Lukasik and R. Bogel-Lukasik. Ionic liquids as a tool for lignocellulosic biomass fractionation. *Sustain. Chem. Process.*, 2013, 1, 3.
36. S. P. S. Chundawat, V. Balan, L. da Costa Sousa and B. E. Dale. Thermochemical pretreatment of lignocellulosic biomass. in *Bioalcohol Production-Biochemical Conversion of Lignocellulosic Biomass.*, ed. J. Waldron, Woodhead Publishing Ltd., (CRC Press), 2010, vol. 3, p. 24–72.
37. M. J. Taherzadeh and K. Karimi. Pretreatment of lignocellulosic wastes to improve ethanol and biogas production: a review. *Int. J. Mol. Sci.*, 2008, **9**, 1621–1651.
38. Y. Zheng, Z. Pan and R. Zhang. Overview of Biomass Pretreatment for Cellulosic Ethanol Production. *Int. J. Agric. Biol. Eng.*, 2009, **2**, 51–69.
39. J. M. Lee, H. Jameel and R. A. Venditti. One and Two Stage Autohydrolysis Pretreatments for Enzyme Hydrolysis of Coastal Bermuda Grass to Produce Fermentable Sugars. *Bioresources*, 2010, **5**, 1496–U6.
40. F. Carvalheiro, T. Silva-Fernandes, L. C. Duarte and F. M. Gírio. Wheat straw autohydrolysis: process optimization and products characterization. *Appl. Biochem. Biotechnol.*, 2009, **153**, 84–93.
41. A. a Modenbach and S. E. Nokes. The use of high-solids loadings in biomass pretreatment--a review. *Biotechnol. Bioeng.*, 2012, **109**, 1430–42.
42. L. J. Jönsson, B. Alriksson and N.-O. Nilvebrant. Bioconversion of lignocellulose: inhibitors and detoxification. *Biotechnol. Biofuels*, 2013, **6**, 16.
43. O. Akpinar, K. Erdogan and S. Bostanci. Production of xylooligosaccharides by controlled acid hydrolysis of lignocellulosic materials. *Carbohydr. Res.*, 2009, **344**, 660–666.
44. A. A. Achary and S. G. Prapulla. Xylooligosaccharides (XOS) as an Emerging Prebiotic: Microbial Synthesis, Utilization, Structural Characterization, Bioactive Properties, and Applications. *Compr. Rev. Food Sci. Food Saf.*, 2011, **10**, 2–16.

45. M. J. . Vázquez, J. L. Alonso, H. Domínguez and J. C. Parajó. Xylooligosaccharides: manufacture and applications. *Trends Food Sci. Technol.*, 2000, **11**, 387–393.
46. Gupta Praveen Kumar, A. Pushpa and H. Prabha. A review on xylooligosaccharides. *Int. Res. J. Pharm.*, 2012.
47. P. R. Bernardo. Optimização de Pré-tratamentos Hidrotérmicos para a Hidrólise Selectiva das Hemiceluloses de Bagaço de Azeitona Extractado. FCT-UNL, 2011.
48. A. Demirbas. Supercritical fluid extraction and chemicals from biomass with supercritical fluids. *Energy Convers. Manag.*, 2001, **42**, 279–294.
49. R. L. Mendes, B. P. Nobre, M. T. Cardoso, A. P. Pereira and A. F. Palavra. Supercritical carbon dioxide extraction of compounds with pharmaceutical importance from microalgae. *Inorganica Chim. Acta*, 2003, **356**, 328–334.
50. G. Brunner. Supercritical fluids: technology and application to food processing. *J. Food Eng.*, 2005, **67**, 21–33.
51. J. R. Williams, A. A. Clifford and S. H. R. Al-Saidi. Supercritical fluids and their applications in biotechnology and related areas. *Mol. Biotechnol.*, 2002, **22**, 263–286.
52. J. W. King, K. Srinivas, O. Guevara, Y. W. Lu, D. F. Zhang and Y. J. Wang. Reactive high pressure carbonated water pretreatment prior to enzymatic saccharification of biomass substrates. *J. Supercrit. Fluids*, 2012, **66**, 221–231.
53. K. L. Toews, R. M. Shroll, C. M. Wai and N. G. Smart. pH-Defining equilibrium between water and supercritical CO₂ - Influence on SFE of organics and metal-chelates. *Anal. Chem.*, 1995, **67**, 4040–4043.
54. N. Weiss, J. Börjesson, L. S. Pedersen and A. S. Meyer. Enzymatic lignocellulose hydrolysis: Improved cellulase productivity by insoluble solids recycling. *Biotechnol. Biofuels*, 2013, **6**, 5.
55. N. Mosier, C. Wyman, B. Dale, R. Elander, Y. Y. Lee, M. Holtzapple and M. Ladisch. Features of promising technologies for pretreatment of lignocellulosic biomass. *Bioresour. Technol.*, 2005, **96**, 673–86.
56. E. P. S. Bon and M. A. Ferrara. Bioethanol Production via Enzymatic Hydrolysis of Cellulosic Biomass. *Biotechnology*, 2010, 1–11.
57. V. Arantes and J. N. Saddler. Access to cellulose limits the efficiency of enzymatic hydrolysis: the role of amorphogenesis. *Biotechnol. Biofuels*, 2010, **3**, 4.
58. M. T. H. Li Zhu, Jonathan P. O'Dwyer, Vincent S. Chang, Cesar B. Granda. Structural features affecting biomass enzymatic digestibility. 2008, **99**, 3817–3828.
59. J. Maclellan. Strategies to Enhance Enzymatic Hydrolysis of Cellulose in Lignocellulosic Biomass. *Biotechnology*, 2010, **6**, 31–35.
60. Y.-H. Percival Zhang, M. E. Himmel and J. R. Mielenz. Outlook for cellulase improvement: screening and selection strategies. *Biotechnol. Adv.*, 2006, **24**, 452–81.

61. M. J. Taherzadeh and K. Karimi. Enzyme-based hydrolysis processes for ethanol from lignocellulosic materials: a review. *Bioresour. Technol.*, 2007, **2**, 707–738.
62. S. P. Magalhães da Silva, A. R. C. Morais and R. Bogel-Lukasik. The CO₂-assisted autohydrolysis of wheat straw. *Green Chem.*, 2014, **16**, 238.
63. G. P. van Walsum and H. Shi. Carbonic acid enhancement of hydrolysis in aqueous pretreatment of corn stover. *Bioresour. Technol.*, 2004, **93**, 217–26.
64. N. R. E. A. Sluiter, B. Hames, R. Ruiz, C. Scarlata, J. Sluiter and D. Templeton. National Renewable Energy Laboratory - NREL. 2006.
65. H. K. Fernand G. Hurtubise. Classification of fine structural characteristics in cellulose by infrared spectroscopy. Use of potassium bromide pellet technique. 1960, **32**, 177–181.
66. K. S. and J. W. K. R. T. Dhamdere. Carbochemicals Production from Switchgrass using Carbonated Subcritical Water at High Temperatures. in *10th International Symposium on Supercritical Fluids, San Francisco 2012*.
67. R. El Hage, L. Chrusciel, L. Desharnais and N. Brosse. Effect of autohydrolysis of *Miscanthus x giganteus* on lignin structure and organosolv delignification. *Bioresour. Technol.*, 2010, **101**, 9321–9329.
68. M. Chena. Autohydrolysis of *Miscanthus x giganteus* for the production of xylooligosaccharides (XOS): Kinetics, characterization and recovery. *Bioresour. Technol.*, 2014, **155**, 359–365.
69. G. P. van Walsum. Severity function describing the hydrolysis of xylan using carbonic acid. *Appl. Biochem. Biotechnol.*, 2001, **91**, 317–329.
70. R. C. McWilliams and G. P. van Walsum. Comparison of aspen wood hydrolysates produced by pretreatment with liquid hot water and carbonic acid. *Appl. Biochem. Biotechnol.*, 2002, **98-100**, 109–121.
71. O. Pfohl, S. Petkov and G. Brunner. Usage of PE—A Program to Calculate Phase Equilibria. *Technische Universität Hamburg-Harburg, Hamburg, Germany 1998*.
72. C. F. Moniz P, Pereira H, Quilhó T. Characterisation and hydrothermal processing of corn straw towards the selective fractionation of hemicelluloses. *Ind. Crops Prod.*, 2013, **50**, 145–153.
73. F. Carvalheiro, M.P. Esteves, J.C Parajó, H. Pereira and F.M. Gírio. Production of oligosaccharides by autohydrolysis of brewery's spent grain. *Bioresour. Technol.*, 2004, **91**, 93–100.
74. F. Carvalheiro, T. Silva-Fernandes, L. C. Duarte and F. M. Gírio. Wheat straw autohydrolysis: process optimization and products characterization. *Appl. Biochem. Biotechnology*, 2009, **153**, 84–93.
75. G. P. van Walsum and H. Shi. Carbonic acid enhancement of hydrolysis in aqueous pretreatment of corn stover. *Bioresource Technology. Bioresour. Technol.*, 2004, **93**, 217–226.

76. T. Rogalinski, T. I. And and G. Brunner. Hydrolysis of lignocellulosic biomass in water under elevated temperatures and pressures. *J. Supercrit. Fluid.*, 2008, **47**, 54–63.
77. M. Taniguchi, H. Suzuki, D. Watanabe, K. Sakai, K. Hoshino and T. Tanaka. Evaluation of pretreatment with *Pleurotus ostreatus* for enzymatic hydrolysis of rice straw. *J Biosci Bioeng*, 2005, **100**, 637–643.
78. W. C. Yang B. Effect of xylan and lignin removal by batch and flowthrough pretreatment on the enzymatic digestibility of corn stover cellulose. *Biotechnol Bioeng.*, 2004, **86**, 88–95.
79. A. M. da C. Lopes, K. João, D. Rubik, E. Bogel-Lukasik, L. C. Duarte, J. Andreus and R. Bogel-Lukasik. Pre-treatment of lignocellulosic biomass using ionic liquids: Wheat straw fractionation. *Bioresour. Technol.*, 2013, **142**, 198–208.
80. S. C. Corgie, H. M. Smith and L. P. Walker. Enzymatic Transformations of Cellulose Assessed by Quantitative High-Throughput Fourier Transform Infrared Spectroscopy (QHT-FTIR). *Biotechnol. Bioeng.*, 2011, **108**, 1509–1520.
81. D. Ciolacu, F. C. And and V. I. Popa. Amorphous cellulose structure-structure and characterization cellulose. *Cell. Chem. Technol.*, 2011, **45**, 13.21.
82. N. Sarkar, S. K. Ghosh, S. Bannerjee and K. Aikat. Bioethanol production from agricultural wastes: An overview. *Renew. Energy*, 2012, **37**, 19–27.
83. M. Stamenic, I. Zizovic, R. Eggers, P. Jaeger, H. Heinrich, E. Roj and D. Skala. Swelling of plant material in supercritical carbon dioxide. *J. Supercrit. Fluid*, 2010, **52**, 125–133.
84. N. Narayanaswamy, A. Faik, D. J. Goetz and T. Y. Gu. Supercritical carbon dioxide pretreatment of corn stover and switchgrass for lignocellulosic ethanol production. *Bioresour. Technol*, 2011, **102**, 6995–7000.
85. Miao Gao, Feng Xu, Shurong Li, Xiaoci Ji, Sanfeng Chen and Dequan Zhang. Effect of SC-CO₂ pretreatment in increasing rice straw biomass conversion. *Biosyst. Eng.*, 2010, **106**.
86. Y. Zhao, Y. Wang, J.Y. Zhu, A. Raqauskas and Y. Deng. Enhanced enzymatic hydrolysis of spruce by alkaline pretreatment at low temperature. *Biotechnol. Prog.*, 2008, **6**, 1320-1328.
87. T. Benazzi, S. Calgaroto, V. Astolfi, C.D. Rosa, J.V. Oliveira and M.A. Mazutti. Pretreatment of sugarcane bagasse using supercritical carbon dioxide combined with ultrasound to improve the enzymatic hydrolysis. *Enzym. Microb. Tech.*, 2013, **52**, 247–250.
88. R. Corrales, F. Mendes, C. Perrone, C. Sant'Anna, W. Souza, Y. Abud, E. Bon and V. Ferreira-Leitão. Structural evaluation of sugar cane bagasse steam pretreated in the presence of CO₂ and SO₂. *Biotechnol. Biofuels*, 2012, **5**.
89. Y. Z. Zheng and T. G. Tsao. Avicel hydrolysis by cellulase enzyme in supercritical CO₂. *Biotechnol. Lett.*, 1996, **18**, 451–454.
90. R. Alinia, S. Zabihi, F. Esmailzadeh and J. Kalajahi. Pretreatment of wheat straw by supercritical CO₂ and its enzymatic hydrolysis for sugar production. *Biosyst. Eng.*, 2010, **107**, 61–66.

91. K. H. Kim and J. Hong. Supercritical CO₂ pre-treatment of lignocellulose enhances enzymatic cellulose hydrolysis. *Bioresour. Technol.*, 2001, **77**, 139–144.
92. V. P. Puri and H. Mammers. Explosive pretreatment of lignocellulosic residues with high-pressure carbon dioxide for the production of fermentation substrates. *Biotechnol. Bioeng.*, 1983, **25**, 3149–3161.
93. T. C. Hsu, G. L. Guo, W. H. Chen and W. S. Hwang. Effect of dilute acid pretreatment of rice straw on structural properties and enzymatic hydrolysis. *Bioresour. Technol.*, 2010, **101**.
94. B. Um, M. Karim and L. Henk. Effect of sulfuric and phosphoric acid pretreatments on enzymatic hydrolysis of corn stover. *Appl. Biochem. Biotechnol.*, 2003, **105**, 115–125.
95. H. Zhang and S. Wu. Subcritical CO₂ pretreatment of sugarcane bagasse and its enzymatic hydrolysis for sugar production. *Bioresour. Technol.*, 2013, **149**, 546–550.

7. Appendix

Annex A – Determination of the partial pressure of CO₂

The partial pressure of CO₂ was determined using the Henry Law:

Equation 7.1

$$p_{CO_2} = k_H \cdot x_{CO_2}$$

Where,

p_{CO_2} - Partial pressure of CO₂ in water

x_{CO_2} - Solubility of CO₂ in water

k_H – Henry's constant

The k_H values were obtained through the Figure 7.1 presented below.

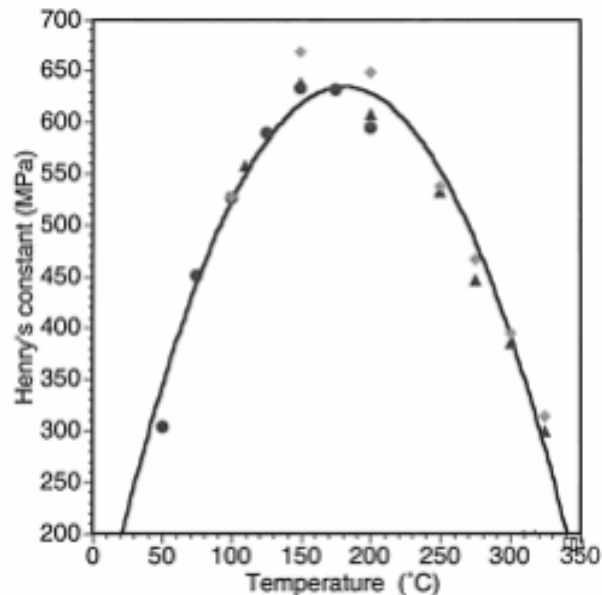


Figure 7.1 – Values for Henry's constant.

G.H. Van Walsum. Severity function describing the hydrolysis of xylan using carbonic acid. *Applied Biochemistry and Biotechnology*, 2001, 91-93, 317-329.

The values of CO₂ solubility in water were obtained from:

Zhenhao Duana and Rui Sun. An improved model calculating CO₂ solubility in pure water and aqueous NaCl solutions from 73 to 533 K and from 0 to 2000 bar. *Chemical Geology*, 2003, **193**, 257-271.

Annex B – Data for the determination of CO₂ density

Table 7.1 – Data for determination of density of CO₂ using the PR-EOS equation, as well as the number of moles of CO₂.

$CS_{p_{CO_2}}$	-3.32	-2.70	-2.43	0.08	-0.48	-0.42	-0.33	-0.13	-0.09	0.00	0.02	0.11	0.19
T_0 (°C) ^a	26.0	26.0	26.0	27.0	26.0	16.0	18.5	16.0	19.5	15.0	22.0	20.0	16.5
p_{CO_2} (bar)	0.0	30.0	60.0	44.76	15.03	14.9	30.0	54.1	30.0	29.9	0.0	44.9	53.1
ρ_{CO_2} (kg·m ⁻³)	0	64	241	109.6	29.20	30.31	66.87	815.34	66.4	69.1	0.0	118.6	809.3
Headspace ^b (mL)	435.0	435.0	435.0	435.1	435.0	490.0	490.0	489.9	436.0	489.9	436.0	490.1	490.0
n_{CO_2} (mol)	0.00	0.63	2.38	1.08	0.29	0.34	0.74	9.08	0.66	0.77	0.00	1.32	9.01

^aTemperature at the time of pressurisation; ^bFree volume in the reactor

Annex C – Determination of feedstock and solid residues

The concentrations of glucose, xylose, arabinose and acetic acid resultant from quantitative acid hydrolysis of the feedstock and solid residues were used to calculate the glucan, xylan, arabinan and acetyl groups percentage, respectively (Eq. 7.2 to 7.5). The acid insoluble residue, after ashes correction, allowed the calculation of Klason Lignin (Eq. 7.6).

Because of the little percentage of sugars degradation in quantitative acid hydrolysis, correction factors are introduced to correct losses. According to Browning those losses are 2.6% for glucose, 8.8% for xylose and 4.7% for arabinose. Based on these percentages it is possible to calculate the correction factors (F) which will allow correcting all the determinations.

Equation 7.2

$$Gn = F \cdot \frac{100}{1005} \cdot \frac{162}{180} \cdot \frac{Glc \cdot W_{sol}}{S}$$

Equation 7.3

$$Xn = F \cdot \frac{100}{1005} \cdot \frac{132}{150} \cdot \frac{Xyl \cdot W_{sol}}{S}$$

Equation 7.4

$$Arn = F \cdot \frac{100}{1005} \cdot \frac{132}{150} \cdot \frac{Ara \cdot W_{sol}}{S}$$

Equation 7.5

$$GAc = F \cdot \frac{100}{1005} \cdot \frac{60}{61} \cdot \frac{Ac \cdot W_{sol}}{S}$$

Equation 7.6

$$LK = \frac{AIR - Ash}{S} \cdot 100$$

Knowing that:

- Gn, Xn, Arn, GAc e LK are the percentages (g·100g solid⁻¹) of glucan, xylan, arabinan, acetyl groups and Klason Lignin, respectively;
- F it is the correction factor. For example, for glucan:

Equation 7.7

$$F = \frac{1}{1-0.026} = 1.027$$

- Wsol and S are the weight (g) of the solution and dry sample used in the assay, respectively.
- AIR and Ash are the weight (g) of acid insoluble residue and ash in the sample, respectively.
- Glc, Xyl, Ara and Ac are the concentrations (g·L⁻¹) of glucose, xylose, arabinose and acetic acid in the liquors, respectively.

Annex D – Determination of percent digestibility of cellulose

The glucose concentration determined by HPLC is corrected for hydration multiplying it by 0.9, due to the water molecule added upon hydrolysis of cellulose polymer. Then, the percentage digestion is determined through the equation 7.8.

Equation 7.8

$$\% \text{ digestion} = \frac{\text{grams cellulose digested}}{\text{grams cellulose added}} \cdot 100$$

Annex E – Phenolics concentration determination

Solutions preparation

Gallic acid stock solution 0.6 g·L⁻¹

0.0300 g of gallic acid were weighted and diluted in ultra-pure water. The total solution volume was 50 mL in a volumetric flask. Commercial reagent was considered as pure, thus no correction was done to determine the real purity.

Sodium carbonate stock solution 7.5% (w·v⁻¹)

18.75 g of sodium carbonate were weighted and dissolved in ultra-pure water. The total volume of solution was 250 mL and it was prepared in a volumetric flask.

Folin-Ciocalteu 1/10 (v·v⁻¹)

25 mL of commercial Folin Ciocalteu reagent was dissolved in ultra-pure water. The total volume of solution was 250 mL and it was prepared in a volumetric flask.